ABSTRACT

HO, PHU NGUYEN. Intelligent Energy Distribution for Series PHEVs Using Optimal Driving Patterns Determined via a Genetic Algorithm. (Under the direction of Dr. Eric Klang.)

This research introduces an intelligent energy distribution scheme for series Plug-in Hybrid Electric Vehicles (PHEVs) that incorporates the complexity of human driving behavior. Hybrid Electric Vehicles (HEVs) have been shown to improve fuel economy, reduce vehicle emissions and maintain drivability by incorporating electric motors into the drivetrain and a battery as a secondary power source. HEVs ability to meet driver demands by distributing load through multiple power sources yields significant benefits over conventional Internal Combustion Engine (ICE) vehicles. However, due to the highly complex system design and vehicle architecture of hybrid vehicles, sophisticated Energy Management Strategies (EMS) are required to optimize vehicle performance. Currently, the power management system for HEVs is based on static thresholds optimized on a fixed drive cycle for a given vehicle.

This research introduces an adaptive control method for EMS by adapting the upper and lower State-of-Charge (SOC) limits. By utilizing a Genetic Algorithm (GA) optimization method to determine the optimal driving patterns offline, an optimal EMS can be derived to maintain an effective control algorithm for the vehicle in real time. The aim of the EMS is to reduce fuel consumption while maintaining vehicle performance through an adaptive control strategy by adjusting the energy distribution between the ICE and the Energy Storage System

(ESS). The adaptive control strategy for a series PHEV was demonstrated in this research by incorporating determined optimal driving patterns to improve vehicle performance and efficiency. A simulation of the adaptive control strategy using drive cycles (US06) specified by the Environmental Protection Agency (EPA) showed improvement in fuel economy up to 15 percent. This framework led to better vehicle performance while accomplishing a reduction in fuel consumption, a reduction in ESS thermal generation and an increase in usable power capacity over a wider range of SOC.

Intelligent Energy Distribution for Series PHEVs Using Optimal Driving Patterns Determined via a Genetic Algorithm

by
Phu Nguyen Ho

A dissertation submitted to the Graduate Faculty of
North Carolina State University
in partial fulfillment of the
requirements for the Degree of
Doctor of Philosophy

Mechanical Engineering

Raleigh, North Carolina

2013

APPROVED BY:

_____	_____
Dr. Eric Klang Chair of Advisory Committee	Dr. James Rigsbee
_____	_____
Dr. Jeffrey Eischen	Dr. Scott Ferguson

DEDICATION

To my mother Nga and father Duy Ho.

BIOGRAPHY

Phu Nguyen Ho's academic interests include the energy efficiency of dynamic systems, model reduction, embedded systems, system optimization, motorsports and advanced materials. His current research focuses on intelligent energy distribution for series hybrid electric vehicles using optimal driving patterns determined via a genetic algorithm. His fascination in motorsports and embedded systems have steered him into automotive research and development, with three years as a senior technical contributor for Wolfpack Motorsports, a university-sponsored formula SAE racing team.

He holds a B.S. and M.S. in Mechanical Engineering from North Carolina State University and has worked previously as an intern and project planner at BMW Manufacturing Co., LLC. As an intern he received the BMW iPower award in recognition of an innovative energy saving idea that improved signal processing.

ACKNOWLEDGMENTS

First, I would like to thank the U.S. Department of Energy, General Motors, Argonne National Laboratory, EcoCAR2, and all of the sponsors for making this research possible. Next, I would like to thank my advisor, Dr. Eric Klang for his guidance, encouragement and philosophy throughout the duration of this research. Additionally, specials thanks go to my committee members, Dr. James Rigsbee, Dr. Jeffrey Eischen, and Dr. Scott Ferguson for their support, inspirations and wisdoms. Last but not least, a huge thanks to Kevonte Mitchell for helping to edit this document. Finally, I would like to express my gratitude to my family, extended family and friends for being supportive and encouraging throughout my endeavors.

TABLE OF CONTENTS

LIST OF TABLES

LIST OF FIGURES

NOMENCLATURE

AC	=	alternating current
$ADVISOR$	=	Advanced Vehicle Simulator
ANN	=	artificial neural network
BCM	=	battery control module
CAN	=	controller area network
CD	=	charge depleting
CS	=	charge sustaining
d	=	distance
DC	=	direct current
DOH	=	degree of hybridization
ECU	=	engine control unit
E_g	=	resistance heating
EMS	=	energy management strategies
EPA	=	environmental protection agency
ESS	=	energy storage system
$f(t_i)$	=	fuel consumption objective function
$f(x_i)$	=	objective function
GA	=	genetic algorithm
$G_c(w)$	=	lag controller
$GM\ LAN$	=	single wire low speed CAN

$G(t_i)$ = distance constraints

$G(x_i)$ = constraints

HEV = hybrid electric vehicle

$HS\ CAN$ = high speed CAN

HV = high voltage

i = overall transmission ratio

I = electric current

ICE = internal combustion engine

K_w = lag controller gain value

$\dot{m}$ = mass fuel flow rate

MPG = mile per gallon

$\dot{m}(v_i)$ = mass fuel flow rate at vehicle speed

n = engine speed

P_{EM} = rated power for electric traction motor

$PHEV$ = plug-in hybrid electric vehicle

P_{ICE} = rated power for internal combustion engine

r = effective tire radius

R_e = electrical resistance

SOC = state of charge

SOH = state of health

t = time

v = vehicle speed

w_p = lag controller pole value

w_z = lag controller zero value

Chapter 1
Introduction

The high demand for alternative energies has led to the emergence of Hybrid Electric Vehicles (HEVs) in the automotive industry. HEVs have been shown to have improved fuel economy and reduced vehicle emissions, while maintaining drivability. This efficiency is achieved by incorporating electric motors into the drivetrain and a battery as a secondary power source. The HEV's ability to meet driver demands by distributing load through multiple power sources yields significant benefits over conventional Internal Combustion Engine (ICE) vehicles. With the added complexity of the Energy Storage System (ESS) and other subsystems in HEVs more advanced control strategies are required to manage the energy distribution between multiple energy sources. Yet, to date, there is no past research on improving vehicle fuel efficiency that considers an adaptive control strategy for series Plug-in Hybrid Electric Vehicles (PHEVs) using optimal driving patterns determined via a genetic algorithm.

The concept of HEVs for improving fuel efficiency has been around for generations. Researchers have looked at various ways to improve vehicle efficiency using different

methodologies. Micro-hybrid vehicles with auto-start-stop based on the conventional 14V electrical system with brake energy regeneration have been shown to reduce fuel consumption by three percent (Shaeck et al. 2009). Others have studied advanced control strategies using optimization methods such as the stochastic fuzzy controller, artificial neural networks and genetic algorithms to maintain vehicle performance and reduce fuel consumption (Junghwan et al. 2010; Paladini et al. 2007). Barsali et al. (2004) proposed an algorithm to reduce fuel consumption (1.6-5%) for HEVs through the forecasting of future vehicle load. Other researchers have looked at on-board estimation of the State-of-Charge (SOC) using methods such as equivalent resistor-capacitor circuits and extended Kalman filters to estimate the battery state of health; all aiming to better control the energy distribution for HEVs (Hu et al. 2011; Junghwan et al. 2010; Plett 2004). Nonetheless, while employing complex control algorithms which are known to improve the fuel economy of passenger cars, it is critical to understand how driving styles can affect fuel economy to improve vehicle efficiency.

One factor contributing to vehicle inefficiency is an individual's driving style. Driving style can have a significant impact on fuel consumption, but it is often unclear how one should drive to get the optimal fuel efficiency (Hooker 1988). Studies have shown that aggressive driving based on sudden acceleration and deceleration results in fuel wastage of approximately 33 percent at high speeds such as highway travel and about 5 percent at lower speeds around town (as quoted in Sahoohi 2009). Other researchers have examined driving style assistance platforms called smart systems (Hannan et al. 2008; Saerens et al. 2009; Schicbahn et al. 2008). Yet, while smart systems such as intelligent speed adaptation give

feedback to the driver and provide speed limitations, they are mainly designed for safety and comfort (Saerens et al. 2009). A clear understanding of driving patterns can lead to better understanding of real-world vehicle performance and ultimately a more efficient vehicle control strategy.

One tool that can help understand driving patterns is the Genetic Algorithm (GA). In recent years, GAs have become a popular optimization tool for many areas of research, including automotive engineering. Researchers in electrical and mechanical engineering have shown that GAs provide effective solutions to complex problems such as the traveling salesman, engine parameters optimization and active suspension control for vehicles (Chiou and Liu 2009; Fujita et al. 1998; Moon et al. 2002). The present research introduces an intelligent energy distribution scheme for series PHEVs by using optimal driving patterns determined via a genetic algorithm to improve fuel economy. The remainder of this manuscript will be arranged into two main parts to help organize the flow of this research:

Part 1 - Model-based determination of optimal driving patterns via a genetic algorithm

Chapter 3 goes into details of how the numerical model was developed to determine the optimal driving patterns using a genetic algorithm. An experimental setup of a GM Ecotec engine test bed was developed to collect the necessary data to serve as input for the numerical model. Finally, the result of the determined driving patterns is evaluated against two Environmental Protection Agency (EPA) predefined drive cycles (FTP and UDDS) as a benchmark of fuel consumption. These evaluations provide the basic understanding of

driving patterns, which will allow us to develop an adaptive control strategy for a series PHEV that improves vehicle fuel efficiency.

Part 2 – Adaptive control strategy development for series PHEVs

Chapter 4 introduces an adaptive control strategy for series PHEVs, which is derived from the optimal driving patterns obtained in *Part 1*. The aim is to reduce fuel consumption while maintaining the system's integrity by adjusting the energy distribution between the ICE and ESS for a series PHEV. The adaptive control strategy is modeled in Simulink and integrated in Advanced Vehicle Simulator (ADVISOR) via MATLAB to evaluate different aspects pertaining to the vehicle performance over a drive cycle.

Further, Chapter 4 evaluates the design of the adaptive control strategy, and the parameters are tuned to meet the desirable performance for a series PHEV. Three parameters are considered: lag controller design, bandwidth parameter, and upper and lower limits ratio, which allows us to see how it affects the ESS SOC and discharge rate. The best performing combination parameters are selected based on the design target and desirable characteristics of the SOC for the ESS.

With the control strategy complete, Chapter 5 looks at the vehicle communication protocol for implementation of the new adaptive control strategy. Taking advantage of the CAN communication protocol, the control strategy was designed to use existing information available on the CAN bus. This alleviates the computational expenses for implementation of the control logics.

1.1 Research Motivation

The motivation of this research is to develop a successful and robust control algorithm to reduce fuel consumption while maintaining vehicle performance and consumer acceptability. To this aim, this research focuses on creating an adaptive control strategy for a series PHEV using determined optimal driving patterns to improve vehicle efficiency. With this framework, the control strategy can be integrated with the existing communication platform (Controller Area Network) in the vehicle with minimal additional computational expense.

HEVs have been shown to have improved fuel economy and reduced vehicle emissions, while maintaining drivability by incorporating electric motors into the drivetrain and a battery as a secondary power source. While parallel and series-parallel HEVs have been well studied for power-splitting, series HEVs remain a challenge at highway speeds due to the inherent nature of low torque of electric machines when operating at high speeds (Zeraoulia et al. 2006).

For this research, a series PHEV is selected as the vehicle architecture, which has the simplest powertrain configuration among different hybrid vehicles. Most beneficial is the ability to operate the ICE at the most efficient point to deliver electric power via the generator to the traction motor or to charge the battery.

Due to the highly complex system design and vehicle architecture of hybrid vehicles, sophisticated Energy Management Strategies (EMS) are required to optimize the vehicle performance and efficiency. Currently, power management systems for series HEVs are

based on static thresholds optimized on a fixed drive cycle for a given vehicle. However, by having an adaptive control strategy that actively governs the ICE active state during a drive cycle, a reduction in fuel consumption can be achieved and potentially improve vehicle performance and battery life.

1.2 Problem Statement

Modern automobiles have evolved into complex mechanical and digital systems that require advanced control strategies to function adequately. Further, the complexity of the recently introduced hybrid vehicle requires an innovative way to obtain greatest efficiency in a system that distributes power requirements across multiple power sources. However, current control strategies with static thresholds may limit the maximum potential of vehicle fuel efficiency. Yet, to date, there is no past research on improving vehicle fuel efficiency that considers an adaptive control strategy for series PHEVs using determined optimal driving patterns via a GA. This research aims to reduce fuel consumption while maintaining vehicle performance through an adaptive control strategy for series PHEVs using optimal driving patterns determined via a GA.

The ideal energy distribution for a series PHEV can be formulated as follows: In order to attain maximum efficiency, there must be a balanced energy distribution between the ICE and ESS that consumes the least amount of fuel. The ICE is assumed to operate at the most efficient point during its active state during a drive cycle to help reduce emissions. However, it is well known that electric traction motors loses torque when operating at high speed, which can be translated into inefficiency when the vehicle operates in electric mode. The question of interest is then: *When do we turn the ICE on and off to get the best fuel efficiency?*

With this in mind, and in order to derive an effective control strategy, it is essential to have insight into individuals' driving patterns (time and speed) along with the power requirements of the electric traction motor. These driving patterns will allow us to determine the vehicle speeds that are least efficient for a series PHEV, and determine how to govern the ICE active state. In this research, the adaptive control strategy is modeled in Simulink in the MATLAB environment, which is the *de facto* design platform in the Control Engineering community, and integrated in ADVISOR (Gladwin et al. 2009). The following aspects will be addressed in this research:

- Driving patterns with the lowest fuel consumption
- Adaptive control strategy for series PHEVs
- Vehicle communication for controls integration

Chapter 2
Literature Review

This chapter provides a brief literature review on the topics of interest pertaining to this research. The chapter is divided into three sections covering topics including vehicle efficiency, controls strategy, and vehicle communication as follows:

Section 2.1 covers topics pertaining to *Part 1* of this research regarding the model-based determination of driving patterns. It addresses the current research in vehicle efficiency and optimization methods. Additionally, Section 2.1 discusses state-of-the-art optimization methods such as GAs and ANNs used to optimize vehicle parameters and control algorithms for vehicle efficiency.

Section 2.2 covers topics pertaining to *Part 2* of this research which deals with the control strategy development for a series PHEV. There, the basics of HEVs along with current research to improve vehicle efficiency are considered. Additionally, the current optimization methods for improve HEVs efficiency will be discussed as well as the importance of the ESS and thermal characteristics in HEVs application.

Section 2.3 covers the topics pertaining to vehicle communication for controls integration. This section considers the power electronics used in *Part 1* along with the micro-

controller used by the NCSU EcoCAR2 team for implementing advanced control algorithms. In addition, the serial communication Controller Area Network (CAN) protocol will be discussed.

2.1 Topics Pertaining to Vehicle Efficiency

As environmental concerns continue to increase, it is imperative to improve fuel efficiency in today's automobiles while maintaining drivability and reducing vehicle emissions (Michalek et al. 2004). Currently, smaller vehicles, including hybrid electric and electric vehicles, are seen as key to the goal of improving fuel economy and lowering greenhouse gases. In this direction, many of the developers of these vehicles have used strategies that focus on altering physical vehicle parameters such as engine downsizing, components optimization and complex control strategies, while research on individual driving styles has received little attention.

Extensive studies have been done on changing the physical vehicle parameters (Fujita et al. 1998; Schwarzkopf et al. 1977; Wloch and Bentley 2004). Wloch and Bentley (2004) have demonstrated the use of genetic algorithms (GAs) to adjust physical parameters on a Formula 1 car to gain vehicle performance. Researchers have looked at ideas such as engine downsizing and the use of forced induction that produces power and torque comparable to the larger, naturally aspirated engine (Springs et al. 2007).

Varesi and Randan (2011) proposed a method to optimize the Degree of Hybridization (DOH) and battery sizing for a parallel HEV using a GA to improve vehicle performance. Others have demonstrated that the use of advanced optimization methods through complex control algorithms, and Artificial Neural Networks (ANNs) to optimize engine parameters including intake runner length, cam phasing and air/fuel ratio can increase efficiency (Wu et al. 2005; Zhao et al. 2011).

These algorithms are seen in the use of multi spray angle fuel injection, dynamics stability controls and even crash detection (Hannan et al. 2008; Hou et al. 2011; Schicbahn et al. 2008). Complex control algorithms in hybrid vehicles have been shown to increase fuel economy, reduce vehicle emissions and maintain drivability by adjusting the energy balance between the ESS and the ICE (Ho and Klang 2013; Hu et al. 2010; Junghwan et al. 2010; Paladini et al. 2007). It is well established that advanced control strategies such as stochastic fuzzy logic controls, ANNs and GAs are shown to improve vehicle performance and reduce fuel consumption (Junghwan et al. 2010; Paladini et al. 2007).

Nonetheless, while altering physical parameters and employing complex control algorithms are known to improve the fuel economy of passenger cars, it is critical to understand how driving styles can affect fuel economy to aid the vehicle design process (Sahoohi 2009). While smart systems such as intelligent speed adaptation give feedback to the driver and provide speed limitations, they are mainly designed for safety and comfort (Saerens et al. 2009).

Genetic algorithms (GAs) have been used to solve complex engineering problems across a wide range of disciplines. Researchers have shown that GAs provide effective solutions to complex problems such as the traveling salesman, engine parameter optimization and active control suspension for vehicles (Chiou and Liu 2009; Fujita et al. 1998; Moon et al. 2002). GAs are powerful optimization schemes which mimic the basic biological mechanisms of reproduction and "survival of the fittest" (Chiou and Liu 2009).

The genetic algorithm is different from the conventional optimization methods in that it starts with an initial set of random solutions called a population (Gen and Cheng 1997). Each individual in the population is a chromosome, which represents a solution to the problem (Gen and Cheng 1997). A population is assigned based on the non-dominated sorting technique to preserve diversity among solutions (Deb et al. 2002).

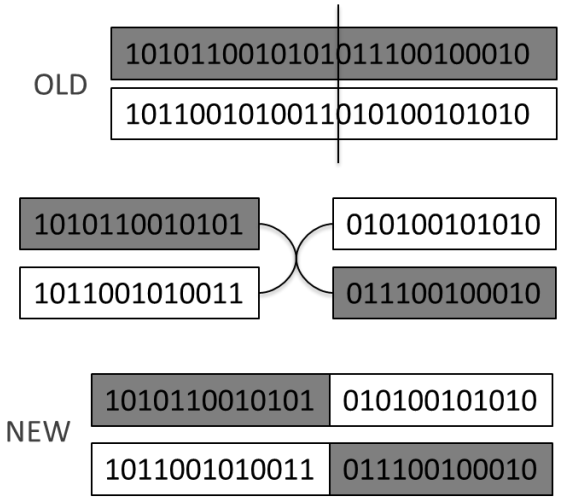

Figure 2.1: Sample GA bit encoding and crossover adapted from Holland 1992.

Figure 2.1 illustrates a bit encoding with a single point crossover for a sample set of a GA solutions (adapted from Holland 1992). The parent solutions (represented in all white or gray) are used to create new children (solutions) that contain parts of both parents. The new solutions are then used in an iterative process with operation such as crossover and mutation to arrive at the optimal solutions. The optimization begins by evaluating the fitness function with the set of the initial population. Then convergence criteria are checked to see if the solutions are optimal solutions. If the convergence criteria are not satisfied, then, genetic operators are applied to find a new set of solutions to carry on to the next generation and the process repeats until the convergence criterion is met (Karen et al. 2006). Figure 2.2 shows a flow diagram of a typical GA optimization scheme.

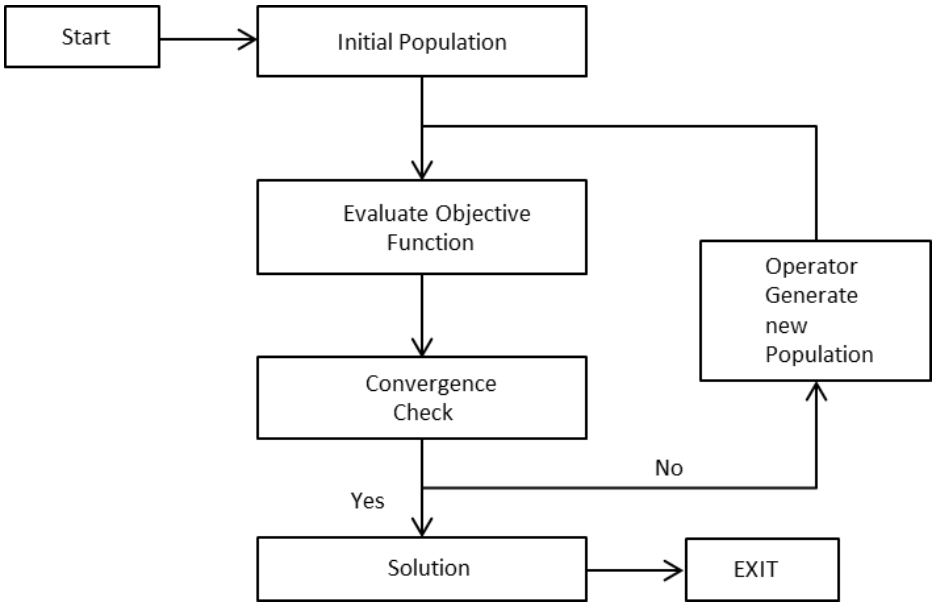

Figure 2.2: Genetic algorithm optimization scheme.

While the process is randomized, it efficiently exploits historical information to speculate on new search points with expected improved performance of the solution (Goldberg 1953). A larger set of initial populations would likely yield a good global optimum solution. In contrast, a smaller population might not have enough good information for reproduction and can produce a suboptimal solution. Hence the trade off—a large population would require more computing time, which could be more expensive.

One advantage of GAs is the stochastic nature of this optimization process to arrive at the optimal solution. The random assignment of solutions or genes to arrive at the best fitness values over different generations allows for diversity among solutions. Operators such as crossover and mutation allows for exploration of the design space from generation to generation to preserved good genetic information. This is critical in an optimization process, where a local minimum could occur in highly complex systems. Moreover, a wide range of highly nonlinear problems can be represented, formulated and solved using GAs. While there are advantages to GAs, researchers are looking for ways to overcome some fundamental challenges associated with this optimization method.

There are challenges associated with using GAs to model complex problems for real-time applications. Fundamentally, GAs are discrete models rather than continuous models, which can be a limitation when working with real-time scenarios. Furthermore, for sufficiently large problems, population size can be a concern due to the intensive computational requirement to solve the problem. As noted by Deb et al., for an objective function with multi-variables, a population size approximately of 500 will yield good

solutions (2002). This will limit in-vehicle implementation of GAs in real-time because of such extensive computational requirement to arrive at the optimal solution.

2.2 Topics Pertaining to Control Strategy

The high demand of alternative energy has led to the emergence of HEVs in the automotive industry. HEVs have been shown to improve fuel economy, reduce vehicle emissions and maintain drivability by incorporating electric motors into the drivetrain and a battery as a secondary power source. The ability to distribute multiple power sources in HEVs to meet driver demands can yield significant benefits over conventional internal combustion engine vehicles. Micro-hybrid vehicles with auto-start-stop based on the conventional 14V electrical system with brake energy regeneration have been shown to reduce fuel consumption by three percent (Shaeck et al. 2009). Many researchers have studied advanced control strategy using optimization methods such as stochastic fuzzy controller, artificial neural network and genetic algorithm to maintain vehicle performance and reduce fuel consumption (Junghwan et al. 2010; Paladini et al. 2007). Barsali et al. (2004) proposed an algorithm to reduce fuel consumption (1.6-5%) for HEVs through the forecasting of future vehicle load. Anderson and Pettit's (1995) work provides a good explanation of individual components and the load-leveling device for HEVs (full details can be found in Anderson and Pettit 1995).

A hybrid vehicle is a vehicle that consists of more than one power sources to provide traction power the vehicle. A HEV is one that uses a combination of conventional energy sources such as a hydrocarbon based fuel in conjunction with a battery to provide propulsion power to the vehicle. There are a number of different hybrid powertrain configurations available and being studied for optimal power flow. Power-splitting techniques for parallel,

series-parallel, parallel through the road and others have been well studied (Bianchi et al. 2010; Liu et al. 2008; Schulz 2004; Syed et al. 2006).

This research focuses on a series PHEV powertrain configuration, where the vehicle can be plugged into the power grid and charged when not in operation. A series PHEV uses the ICE exclusively to power the generator to deliver the electrical power to the high voltage bus or charge the battery. The traction motor is coupled directly to the drivetrain. Two benefits of a series PHEV are the utilization of the ICE at the most efficient point during operation and the simplicity of powertrain configuration. Some of the drawbacks for PHEVs are large capacity batteries requirement which equate to a heavier ESS along with a more stringent cooling system. The most imminent drawback is the inefficiency when the vehicle operates at high speed due to the inherent nature of electric machines' low torque at high speed (Zeraoulia et al. 2006). To alleviate the inadequacy of torque available, the vehicle is designed in a way that the electric drive handles the instantaneous load transient conditions and the engine handles the average road load (Plett 2004). Other researchers have studied advanced control strategy optimization such as stochastic fuzzy controllers, ANNs and GAs to maintain vehicle performance and reduce fuel consumption (Choy et al. 2006; Paladini et al. 2007; Wuet al. 2005; Zhao et al. 2011).

Nonetheless, series HEVs remain a challenge when operating at high speeds due to the inherent nature of electric machines' low torque when operating at high speed (see Zeraoulia et al. 2006 for a complete discussion of electric motor drive issues in HEVs). The most rudimentary control strategy is the thermostat control strategy. The thermostat control

strategies utilize a fixed threshold control for the ICE active state (Anderson and Pettit 1995). While thermostat control strategies are well-known in coolant systems (active when hot), HEVs use similar concept to control the ICE (active when the SOC limit has reached a prescribed limit). The basic thermostat control strategy related to the battery SOC for a typical series HEV is as follows:

- ICE is off when SOC is too high
- ICE is on if power required is higher than what is available
- ICE is on when SOC is too low

Anderson and Pettit's (1995) work provides a good explanation of individual components and the load-leveling device for HEVs along with two extreme control algorithms. The authors discussed the use of the auxiliary power unit (engine) and a load levering device (battery) to accommodate drivers demand and maintain energy efficiency. Specifically, the authors discussed two extremes in the spectrum of control strategies (thermostat control algorithm and power follower). The authors noted that in the thermostat mode, the battery must accommodate all the transient power requirements (Anderson and Pettit 1995). On the other hand, for the power follower, the ICE must operate over its entire range of power levels and perform fast power transient, which can reduce the efficiency and affect emission characteristics (Anderson and Pettit 1995).

For a series PHEV there are three common modes of operation, Charge Depleting (CD), Charge Sustaining (CS) and charging. The vehicle can experience any combination of the three modes in a given drive cycle. There are different control methods that have been

proposed to distribute the energy flow in HEVs. The three modes of operation for series PHEVs are as follows:

Charge Depleting (CD)

The vehicle is in CD mode when the ESS provides all the energy to electric motor as a mean for vehicle propulsion. In the CD mode the ESS is the main energy provider, until it can no longer meet the power demand from the electric motor. As the stored energy in the ESS depleted from the initial SOC to the lower SOC limit, the vehicle enters the Charge Sustaining (CS) mode. This allows the vehicle to utilize the ICE and generator to provide additional energy to drive the vehicle.

Charge Sustaining (CS)

Charge sustaining (CS) mode begins when the ESS SOC falls below a prescribed lower limit and utilize both energy sources (ICE and ESS) to propel the vehicle. In CS mode, the power is drawn mainly from ICE/generator combination and can be assisted from battery as needed. The ICE will be active and directly coupled to the generator providing electrical energy to the high voltage bus, in turn power the electric motor. The electrical energy that is not used to drive the vehicle will then be used to charge the ESS. Once the battery has charged up to a prescribed upper SOC limit or a set condition, the ICE will be turned off and the vehicle re-entered the CD mode. This process repeats for normal operating condition for a typical series HEV.

Charging

Charging is the accumulation of electrical energy in the ESS for future usage. While charging can occur in CD mode, plugging into the electrical grid while the vehicle is not in use through a charger will be the primary mode of charging.

It is critical to have a control strategy that accommodates the different driving modes at various electrical current load conditions. In the case of CD mode, a high ESS discharge rate is required, due to all the electrical power drawn from the ESS. The CS mode on the other hand, drew less electrical current from the ESS but experienced charging during normal operation. A balanced distribution of the energy between the ESS and ICE would give the desirable vehicle performance and can ultimately improve the ESS service life.

Barsali et al. (2004) have proposed a control strategy to minimize fuel consumption of a series HEV based on future load predicting method. The authors proposed a control strategy that required signals that can be used to forecast future vehicle loads. The future vehicle load is derived from the equivalent ripple in the root mean square of the power demand or using sliding average values (Barsali et al. 2004). While improvements in fuel economy were seen, the author suggested that advanced tools such as fuzzy logic and or ANNs could improve the vehicle load forecasting parameter (Barsali et al. 2004).

Many researchers have demonstrated the robustness of GAs to solve and optimize physical vehicle parameters in automotive engineering. Different approaches have been taken with GAs in HEV applications to improve vehicle efficiency and performance. Varesi and

Randan (2011) proposed a method to optimize the Degree of Hybridization (DOH) for a parallel HEV using a GA to improve vehicle performance. Furthermore, the authors noted the selection of the ESS (number of battery modules) depends on two key design factors; maximum charge and discharge capacity during the analysis (Varesi and Ranan 2011). It is worthy to note that the authors found that for a DOH greater than 0.65, the system could not provide the necessary propulsion power (Varesi and Randan 2011). The DOH is defined as:

$$DOH = \frac{P_{EM}}{P_{EM} + P_{ICE}}$$

Where P_{EM} is the rated power for the electric traction motor, and P_{ICE} is the rated power for the ICE. All the parameters in the study were extracted from ADVISOR for a DOH range of 0.3 to 0.65 to formulate the weighed cost function to be used in the GA (Varesi and Randan 2011). By using the GA to optimize these parameters, the authors reported that fuel economy increases as the DOH increases (Varesi and Randan 2011).

Gladwin et al. investigated the stability of rectified Direct Current (DC) output from a three-phase Alternating Current (AC) generator in a series HEV powertrain using genetic programing and GAs (2009). The point of interest is maintaining the ICE at its optimal operating point and to supply a stable DC power to the traction drive inverter (Gladwin et al. 2009). The authors developed a control system that stabilizes the rotational velocity of the engine at its optimal operating point, at the same time rejecting disturbances from the reaction torque of the generator when under load (Gladwin et al. 2009).

Wu et al. (2011) investigated a multi-objective self-adaptive differential evolution (MODASE) algorithm to optimize component sizing in parallel HEVs to increase fuel economy. The authors' goal is to find a set of Pareto optimal solutions to provide alternative schemes to assist the design selection criteria (Wu et al. 2011). The diversity of the Pareto solutions is preserved based on a progressive comparison truncation operator which in turn is based on normalized nearest neighbor (Wu et al. 2011). The authors concluded that the use of MOSADE can provide a useful guide in the HEV development process, particularly in the earlier design phase (Wu et al. 2011).

Others have investigated the use of ANNs to improve vehicle efficiency. ANNs are a mathematical representation of the human brain network intended to imitate the learning and memory instinct of the human brain (Zhao et al. 2011). It stores new 'knowledge' by adjusting the weights of neurons in the ANN. Once the ANN is established the training process can begin (Zhao et al. 2011). At the most basic level, the ANN consists of an input layer, hidden layer, and output layer. It is well known that an ANN is a data-driven 'black-box' model due to the complex hidden layer (Zhao et al. 2011)

The nature of ANNs to handle complex nonlinear systems can be used as a real-time solver. The advantage of ANNs is that only input-output information is needed to handle complex problems. Many researchers have shown that ANNs can solve different complex problems given their ability to provide a good, nonlinear mapping between the inputs and the desired outputs of a system (Choy et al. 2006). Wu et al. have demonstrated the use of an ANN model to simulate and optimize cam phasing in ICEs to maximize the torque output

and reduce emissions while improving fuel economy (Wu et al. 2011). Domenico et al. have demonstrated the use of ANNs for on-line sensor fault detection, isolation and accommodation in automotive engines (2003).

While there are benefits to ANNs, there are drawbacks associated with this method. Due to the learning nature of ANNs, training data is required for a successful implementation. Choy et al. have reported that for some applications, the use of certain online learning methods in an ANN actually yields suboptimal results and inconsistent performance (Choy et al. 2006). The shortcoming is that there is no standard or set of rules when selecting the ANN structure that can guarantee an optimal solution.

Combining the most desirable virtues of ANNs, GAs and fuzzy logic into a hybrid method has shown to be beneficial in certain scenarios. Extended fuzzy C-means and GA have been reported to address the energy flow in a hybrid vehicle (Ippolito et al. 2003). Ippolito et al. (2003) use a multi-objective function and a knowledge-based control system for splitting the vehicle's power demand between the ICE and electric motor for a HEV. The authors noted that conventional methods rely on static thresholds, optimized on a fixed drive cycle and thus cannot handle the highly dynamic and unpredictability of real-life driving conditions (Ippolito et al. 2003). Furthermore, powertrain control problems are known to be very complex due to conflicting requirements in the case of a hybrid vehicle (Ippolito et al. 2003). Not only the functionality and performance of the vehicle is a concern, but the computational power for real-time implementation of the optimization method is also an issue. The authors presented a knowledge-based control strategy that reduces computational

time, which help real-time applications (Ippolito et al. 2003). Since knowledge based systems consist of a database whose structure and size affects the computation directly, the authors utilized a fuzzy-based clustering to mitigate the size of the database (Ippolito et al. 2003). Clustering is a means to partition the data set into smaller manageable sets with similar measures. The multi-objective optimization problem proposed by the authors is to optimize hydrocarbon, carbon monoxide, nitrogen oxide and state-of-charge. With this regard, conflicting objectives are compromised in order to arrive at a solution. The energy flow is managed by generating a database of knowledge for a specific drive cycle through optimization off-line. This data is then stored to be used during real-time. The authors claimed that a processor time reduction up to 85 percent is seen through simulations done in MATLAB with the imposed multi-objective functions and fuzzy c-means clustering (Ippolito et al. 2003).

ANN and GA combinations have been shown to solve highly nonlinear automotive problems. Zhao et al. (2011) have reported an optimization scheme combining ANN and GA to optimize the Atkinson cycle engine. The authors utilized the large expansion ratio of the Atkinson cycle for a hybrid electric vehicle power plant. By taking advantage of the late intake valve closure and the geometric compression ratio, better fuel efficiency can be realized. An engine efficiency model was proposed using ANNs and was trained using data from an engine simulator. In this study, the authors used an ANN model with both single and double hidden-layers to model the engine performance (Zhao et al. 2011). The ANN consists of six inputs variables: engine speed, spark angle, intake valve close, exhaust valve open, geometric compression ratio, and air fuel ratio. A Latin Hypercube Sampling algorithm for

training and test data sets was used in the simulation. The optimization for geometric compression ratio and operating parameters was done using a GA to obtain initial parameters (Zhao et al. 2011). The optimization shown for a combined GA and ANN method for the Atkinson cycle engine produced an improvement in average fuel economy of 8.5 percent for engine speed below 4400 rpm (Zhao et al. 2011).

In addition to reducing fuel consumption, the ESS thermal characteristics play a significant role in HEVs. Many researchers have looked at battery performance under extreme conditions such as high temperature or over voltage and metal oxide cathode degradation that may cause thermal runaway for automotive applications (Roth 2007; Shaeck et al. 2009). Others have looked at on-board estimation of the SOC through methods such as equivalent resistor-capacitor circuits and extended Kalman filters to estimate the battery state of health; all aiming to better control the energy distribution within the vehicle (Hu et al. 2011; Junghwan et al. 2010; Plett 2004). The root of the problem remains that batteries lose performance due to chemical instability when the SOC is near the critical lower limit.

The ESS is a key component in all HEV. The ESS performance is critical for operation, safety and efficiency of a hybrid vehicle. In order for optimal performance and efficiency, the ESS needs to effectively communicate with the entire vehicle during all modes of operation. The battery information required by the vehicle can sometimes be difficult to obtain due the nature of the time variance of the system (Plett 2004). Researchers have looked at methods such as cell balancing through shuffling charge using a switched capacitor, depleting charge with a resistor, adding charge with a DC-DC converter, or

moving charge with a transformer-based system can help improve the battery life and performance (Plett 2004). Plett pointed out for commercial success, the cycle life of the battery must meet or exceed the lifetime of the vehicle (Plett 2004). Cycle life is typically defined as the number of times a battery can be charged and discharged before its capacity falls below 70 or 80 percent of its original capacity (A123 2011). Equally important is the power characteristics at the lower SOC limit of the ESS, where most lithium ion battery technologies lose a significant amount of discharge power (A123 2011).

The Battery Control Module (BCM) monitors and communicates the battery State-of-Health (SOH); SOC, power fade, capacity fade and instantaneous available power to the entire vehicle. These parameters are critical for operation and it is continuously being monitored when the vehicle is in operation. Plett (2004) have demonstrated advanced prediction method of these parameters using the extended Kalman filter for lithium-ion polymer battery parameters estimation for HEV application. The authors noted that Kalman filters are an intelligent—and sometimes optimal—means for estimating the present value of the time-varying "state" of a dynamic system (Plett 2004). The estimation method allows for tracking of the cells' degradation and age changing cell characteristics. This is important in applications such as HEV, where the harsh environment is very demanding on batteries and the BCM, and that precise estimation of some parameters will improve performance and robustness, and ultimately lengthen the useful lifetime of the pack (Plett 2004).

In addition to the accurate prediction of SOH of the ESS, the charge and discharge rate plays a significant role in the battery life. The life of a rechargeable battery is

significantly shortened when the battery is fully charged or discharged (A123 2011; Hu et al. 2011; Plett 2004). Furthermore, overcharging (especially in the case of lithium ion battery) can cause permanent cell damage that leads to catastrophic failure in the form of thermal runaway (A123 2011; Hu et al. 2011; Plett 2004). The ESS charge and discharge rate is a major concern for HEVs where a high electrical current relative to the capacity of the cells is required. The present HEVs can demand up to ± 20 times the capacity rating, C-rate (Plett 2004). Such stringent requirements of electrical current from the traction motor translate into heat generation at the ESS that may cause disastrous failure. The thermal characteristics of the ESS have a significant impact on the performance and life in HEVs where the ESS can experience temperature variations ranging from -30 to 50℃ (Plett 2004).

2.3 Topics Pertaining to Vehicle Communication

This section covers the computing power available onboard a vehicle relating to the hardware and software capability for vehicle communication. As micro-controllers become smaller, faster and cheaper, advanced complex algorithms are integrated in the modern vehicle with little cost or effort. Fully in-house developed controllers as well as original manufactured equipment are seen in automotive engineering development processes. The purpose of the micro-controllers is to carry out the necessary computing requirement onboard the vehicle. Numerous micro-controllers are found in a typical modern vehicle to manage specific tasks such as engine management, powertrain control, antilock-brake system, airbag system, and more. The subsequent section explores the basic understanding of the serial communication

pathway between micro-controllers through the Controller Area Network (CAN) used in modern vehicles.

CAN is a serial communications protocol to support real-time control with a high level of security developed by Robert Bosch GmbH in 1983 (Bosch GmbH 1991). The aim is to improve efficiency of the communication pathway within a system. In automotive application, the electronics components such as engine control units, sensors and subsystems are connected using CAN with bitrates up to 1 Mbps. The CAN standard specification helps unify the communication protocol of these components by different manufactures. The CAN bus topology contains three entities; object layer, transfer layer and physical layer (for a complete CAN standard see Bosch GmbH 1991).

The object layer and transfer layer comprise all of the information broadcasting on the CAN bus. This includes which messages are to be transmitted, acknowledgement of transmitted data and the interface between the messages and hardware. The CAN structure comprises; a start frame, identification, data length code, data field, cyclic redundancy check (CRC) field, acknowledgment (ACK) field and end frame. As a safety measure, the entire data frame is being transmitted through bit stuffing. Figure 2.3 shows the basic layout of a CAN message structure adapted from Bosch GmbH 1991.

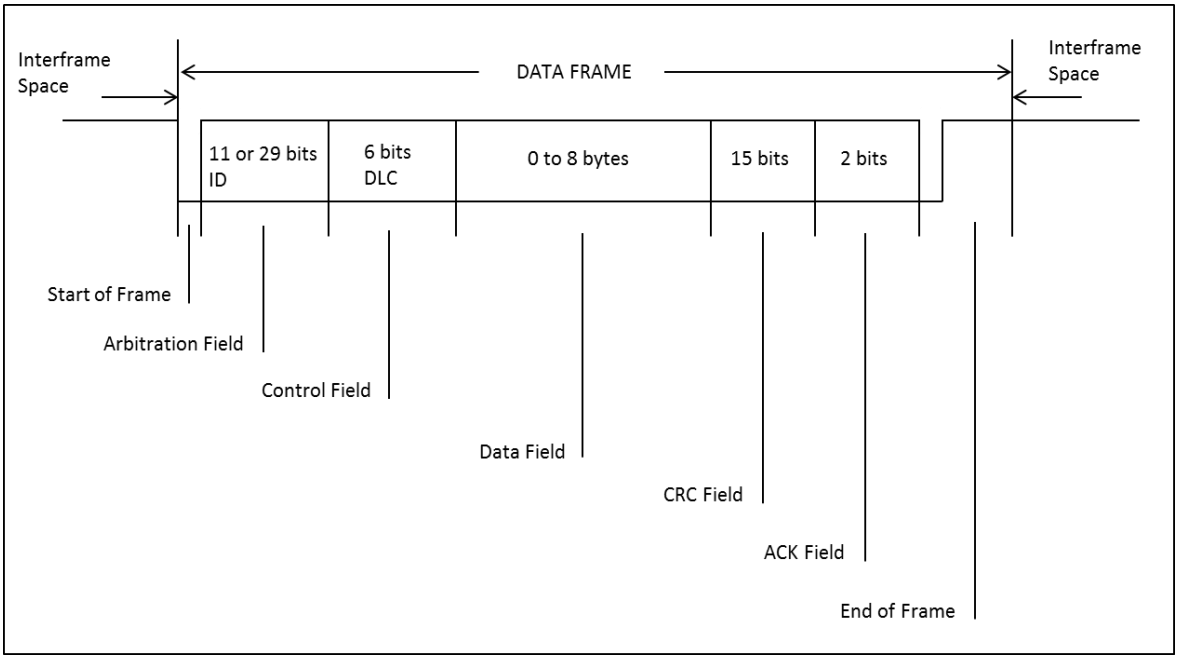

Figure 2.3: CAN data frame adapted from Bosch GmbH 1991.

A single vehicle usually contains multiple CAN buses in order to handle the vast amount of signals required for proper functionality. The 2013 Chevrolet Malibu, used as a test vehicle for the NCSU EcoCAR2 team contains one low speed GM LAN at 33.3 Kbps and 3 high speed (HS) CAN at 500 Kbps (HS CAN, chassis expansion and powertrain expansion). The high speed buses used the 11-bit (standard) identification while the single wire GM LAN utilized a 29-bit extended identification.

The physical layer handles the actual messages in the form of signal and bit representation. To ensure the integrity of the data being transmitted on the bus, the bus length is designed to be less than 25 ft. Furthermore, a pair of twisted wire is used to help reduce the distortion of the signals due to electromagnetic interference. Resistance between the Hi and

Low CAN lines must be 120 Ohm terminated on both ends of the bus for proper signals on the bus. The resistance is needed because the CAN signal is a differential signal. Figure 2.4 illustrates the 120 Ω terminal on both ends of the CAN bus with four CAN devices implemented on the CAN bus.

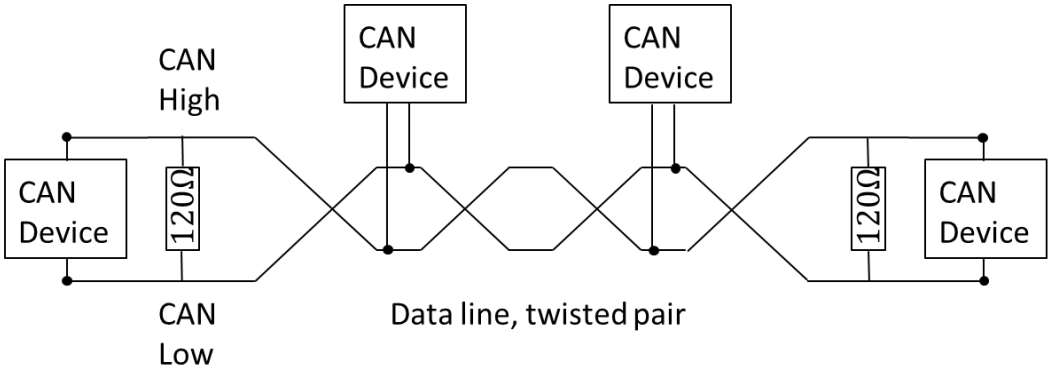

Figure 2.4: CAN devices and bus termination on both ends.

The CAN serial communication allows sensors and subsystems to transmit the information within the vehicle with minimal wire requirement. The CAN protocol provides a simple communication pathway for a highly complex system to transmit information between subsystems. This pathway is critical for the design of HEVs where numerous subsystems (ESS, ICE, generator, battery charger, etc.) require large amounts of communication for normal operation. By having a common communication protocol, various components built by different manufactures can be seamlessly integrated.

A Mototron Engine Control Unit (ECU) is used to develop the GM Ecotec engine to characterize the engine performance in *Part 1*. The ECU has 128 pins and comes with 16-bit

Freescale microprocessors, it proven to be robust and reliably delivering complex control strategy (Woodward 2011). The ECU come with the Freescale MPC565 56 MHz microprocessor with 1M Flash, 548 K RAM, 8K serial EEPROM, 64Kx8 Parallel REPROM operating between 9-32Vdc. The experimental GM Ecotec engine used in this research uses the MPC565 ECU as the stand alone engine controller as shown in Figure 2.5. In the experiment, analogs and digital I/Os, PWM and frequency inputs are used to control and calibrate the engine parameters. The MotoHawk's suite development software and hardware tools were used enabling a rapid development of complex controls for the engine. The engine performance and data were logged using the data acquisition capability onboard the ECU.

Figure 2.5: Mototron engine control module (Woodward 2011).

The NCSU EcoCAR2 team uses a supervisor controller (MicroAutoBoxII) sponsored by dSPACE, to oversee all the communication and controls logic. The MicroAutoBoxII as shown in Figure 2.6 combines the advantages of a rapid prototyping system with those of an automotive ECU (dSPACE 2011). The MicroAutoBoxII can serve as the supervisor

controller in the vehicle under normal operations or can be linked temporarily to a Personal Computer (PC) for reprograming, calibration and data analysis.

Figure 2.6: MicroAutoBoxII 1401/1501 with connector (dSPACE 2011).

One of the benefits of using this controller is that the host interface between the controller and the PC is via the standard Ethernet TCP/IP protocol. Moreover, by having the programing environment through Simulink/MATLAB the controls development process can be done visually rather than through conventional coding. This allows for a quick and simple way to identify errors or control logics during the development process. The MicroAutoBox provides 78-pin analog and digital I/O, PWM, LIN, serial interface, USB connector and two onboard CAN channels suitable for automotive applications. Computationally, the MicroAutoBoxII runs on the ultrafast PPC750GL processor with clock speed of 900 MHz and 16 MB of RAM allowing for high computing environment.

The high computing capability of the MicroAutoBoxII allows for rapid development of complex control strategies in conjunction with CAN communication for prototype vehicles. The NCSU team utilized the existing CAN signals in the stock 2013 Chevrolet Malibu during the development process to seamlessly integrate signals from new components and

subsystems into the vehicle. Understanding of the CAN protocol and Simulink programing environment is critical for the development and implementation of the control strategy for the NCSU hybrid vehicle.

2.4 Summary

Section 2.1 covered the current research on vehicle efficiency, optimization methods and communication protocol used in modern vehicles. Importantly, by altering physical parameters and employing complex control algorithms, improvement in vehicle efficiency can be expected. Heuristic optimization methods such as GAs on the other hand, are important because they allow us to solve a highly nonlinear problem such as determining optimal driving patterns.

Section 2.2 covered the basics of HEVs, vehicle operating modes for series PHEVs, and the thermal characteristics of the ESS and demonstrated that HEVs can yield significant benefits over conventional internal combustion engine vehicles by utilizing multiple power sources. By understanding the different driving modes in a series PHEV, an innovative control strategy to maximize fuel economy can be developed. Further, the charge and discharge rate of the ESS play a critical role in the operation of the HEV and can be managed with an appropriate control strategy to avoid catastrophic failure.

Section 2.3 covered the basics of micro-controllers along with CAN communication protocol. Significantly, the serial communication CAN provides a pathway for information to be transmitted between different subsystems within the hybrid vehicle. Further, with a

common communication protocol, a new control strategy can be implemented with the existing vehicle communication with minimal computing requirements.

With this aspect understood, Chapter 3 proceeds to develop a numerical model utilizing a genetic algorithm optimization method to determine the optimal driving patterns, which is the next step in creating an adaptive control strategy.

Chapter 3
Model-based Determination of Optimal Driving Patterns (Part 1)

Driving style can have a significant impact on fuel consumption, but it is often unclear how one should drive to get the optimal fuel efficiency (Hooker 1988). This chapter introduces a model-based method to determine the optimal driving patterns with the lowest fuel consumption utilizing a GA optimization method. In recent years, GAs have become a popular optimization tool used in engineering to solve complex problems. This is important because it allows us to handle highly nonlinear systems and arrive at an optimal solution.

By combining the robustness of GAs with known engine performance, a numerical model was developed to determine the optimal driving patterns for two scenarios (city and highway). With this in mind, a multi-variable single objective problem is formulated combining experimental engine data from a GM Ecotec engine to determine the optimal driving patterns. Using two EPA drive cycles as benchmarks, a reduction in fuel consumption was seen for the determined driving patterns.

3.1 Experimental Setup

The experimental data from a 2006 General Motors (GM) Ecotec 2.0L supercharged engine is used as input for the numerical model; the data was obtained under the direction of Dr. Richard Gould, where engine performance and fuel efficiency were investigated. This engine utilizes an Eaton M-62 helical roots-type supercharger that can produce a maximum boost pressure of 12 psi (General Motors 2005). In this experiment, the engine is controlled by a standalone ECU by Mototron and is mapped to produce the maximum allowable torque and horsepower for this engine. The engine torque is measured through an Omega load cell, coupled to a Go-power water brake dynamometer. Table 3.1 shows the engine parameters in this experiment. Figure 3.1 shows the experimental setup with the engine coupled to the water brake dynamometer. The data is then logged through the Mototron built-in data acquisition system for analysis. The mass fuel flow rate $\dot{m}_f$ can then be computed from the logged injection timing and fuel rail pressure at different engine speeds.

Table 3.1: GM Ecotec engine parameters used in this experiment.

Engine	2.0L GM Ecotec Supercharged Inline-4
Displacement	121.9 cu in
Bore	3.39 in
Stroke	3.39 in
Compression	9.5:1
Power	205 bhp @ 5600 rpm
Torque	200 ft lbs @ 4400 rpm
Valve train	OHC, 4 Valves per Cyl

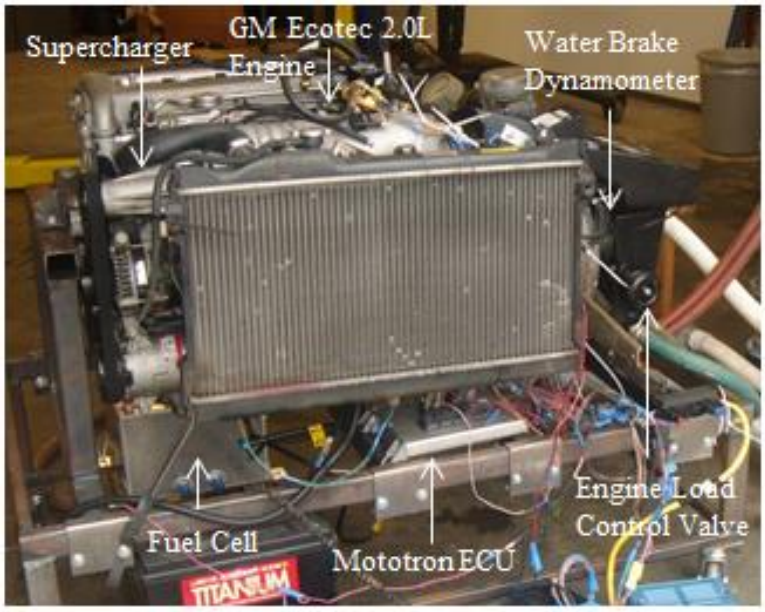

Figure 3.1: Experimental GM Ecotec 2.0L supercharged engine setup with dynamometer and data acquisition system.

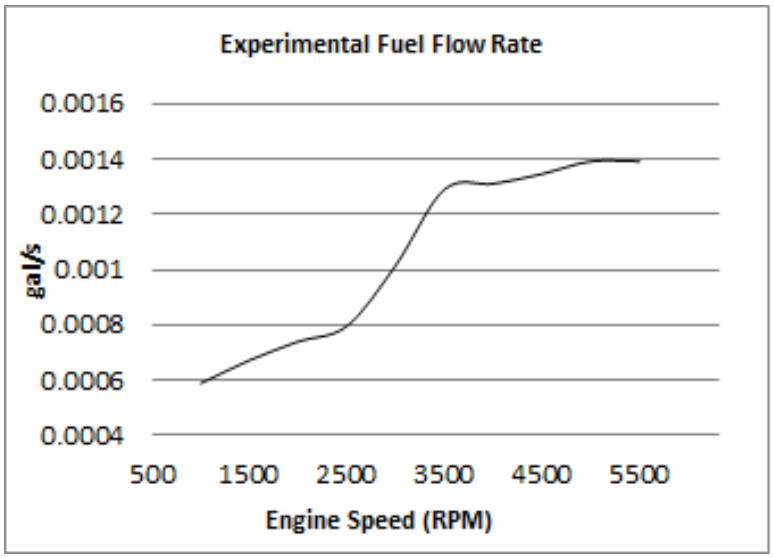

Figure 3.2: Experimental GM Ecotec engine fuel flow rate at 100 percent engine load.

The relationship between the engine speed and vehicle speed is given by (Bosch GmbH 2010).

$$n = \frac{63{,}360 \cdot v \cdot i}{60 \cdot 2\pi r} \tag{1}$$

Where *n* is the engine angular rotation in revolutions per minute (rpm), *v* is the vehicle speed in miles per hour (mph), *i* is the overall transmission ratio between the engine and driven wheels and *r* is the effective tire radius. The overall transmission ratio of 2.88 and effective tire radius of 12.8 inches were used to find the vehicle speed from the known engine speed. While there are many variables involved in a real driving scenario, the vehicle is assumed to operate in the highest gear—5th—throughout the driving duration, holding the power transmission constant.

3.2 Optimization Objective

The objective is to determine the optimal driving patterns with the lowest fuel consumption for a given distance. To achieve maximum fuel efficiency over a given distance a minimum amount of fuel must be consumed. This minimum amount of fuel consumption corresponds to an optimal driving pattern (i.e., $f_{fuel,consumed} \approx \sum_{i=1}^{n} t_i \cdot v_i$, where t_i is time duration and v_i is the vehicle speed). By optimizing these time durations at each driving speed, the optimal driving pattern can be achieved with the lowest fuel consumption. The brake specific

fuel consumption (BSFC) for a given engine is optimal near 80% load, where 80% engine load is assumed for normal driving condition (Bosch GmbH 2010).

3.3 Mathematical Formulation

The standard form of a multivariable objective function is used to model the fuel consumption as shown below. Where x_i is a set of design variables for all real x_i in the subset of *X*, the feasible design space with dimension *n*. The solution would give the minimal value to the objective function $f(x_i)$ subjected to the constraints and boundary conditions (Vanderplaats 2007).

$$\min f(x_i) \tag{2}$$

$$\text{Subject to } G(x_i) \leq 0 \tag{3}$$

$$\text{For } x_i \in X \subseteq \mathbb{R}^n \tag{4}$$

The fuel efficiency model for optimization is as follows:

$$\min f(t_i): \sum_{i=1}^{11} \dot{m}(v_i) \cdot t_i \tag{5}$$

$$Subject\ to\ G(t_i): \sum_{i=1}^{11} v_i \cdot t_i \geq d \tag{6}$$

$$\dot{m}(v_i) = \beta_0 + \beta_1 \cdot v_i + \beta_2 \cdot {v_i}^2 + \beta_3 \cdot {v_i}^3 + \beta_4 \cdot {v_i}^4 + \beta_5 \cdot {v_i}^5 + \beta_6 \cdot {v_i}^6 \tag{7}$$

$$0 \leq t_i \leq \frac{d}{v_i}$$

$$\text{for } i = 1,2,3 \ldots 11 \tag{8}$$

The mass fuel flow rate (gal/hr) as a function of vehicle speed $\dot{m}(v_i)$ is a 6th degree polynomial having the form of Eq. (7). The coefficient β_j for $j = 0,1,2 \ldots 6$, was found from the experimental data using the least squares regression method with $R^2 = 0.998$ ($\beta_j = 0, 0.1954, -0.0065, 0.0001, -6 \times 10^{-7}, 8 \times 10^{-10}, 3 \times 10^{-12}$), where v_i is the vehicle speed (mph) and t_i is the time duration in hours. The speed limits of 20-45 mph for city and 45-70 mph for highway driving are chosen to be the upper and lower bounds, respectively, while *d* is the distance traveled in the two driving scenarios considered: city (low speed, 10 mi distance) and highway (high speed, 100 mi distance). By combining Eq. (7) and Eq. (8), the objective function for city and highway can be obtained as follows:

$$f(t_i)_{city} = \dot{m}(v_{i,city}) \cdot t_{i,city} \tag{9}$$

$$f(t_i)_{hwy} = \dot{m}(v_{i,hwy}) \cdot t_{i,hwy} \tag{10}$$

By minimizing Eq. (9) and Eq. (10) and subjecting them to the constraints, the lowest amount of fuel consumed would yield the optimal driving patterns for both the city and the highway scenarios. A population size of *p* = 500, type = double vector, selection = stochastic uniform, crossover = scattered and stopping tolerance of 1E-6 are used in the MATLAB genetic algorithm solver for both city and highway scenarios.

3.4 Results & Discussion

Figures 3.3 and 3.4 show the time duration spent at each driving speed in order to get the lowest amount of fuel consumption for the city and the highway driving scenarios,

respectively. The most fuel efficient speeds for the city driving scenario were determined to be near 35 and 45 mph because they provided the longest driving duration as shown in Figure 3.3. For the highway scenario, a speed of around 62.5 mph was the most efficient (see Figure 3.4). However, while these three key speeds occurred for the longest duration, transitional speeds are required to achieve the lowest fuel consumption as seen in Figures 3.3 and 3.4. The determined patterns reflect real-world driving conditions for both scenarios, where highway travel is predominately at speeds near 60 mph and common city speed limits are 35 mph and 45 mph. The corresponding fuel economy for the driving patterns in Figures 3.3 and 3.4 are 20 and 26 mile per gallon (MPG), respectively.

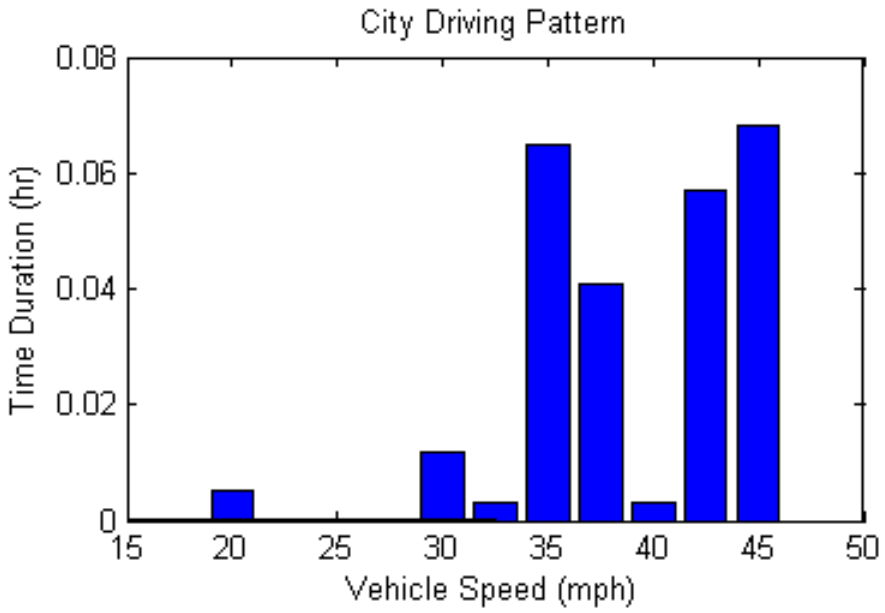

Figure 3.3: GA optimal driving pattern for city scenario with the lowest fuel consumption.

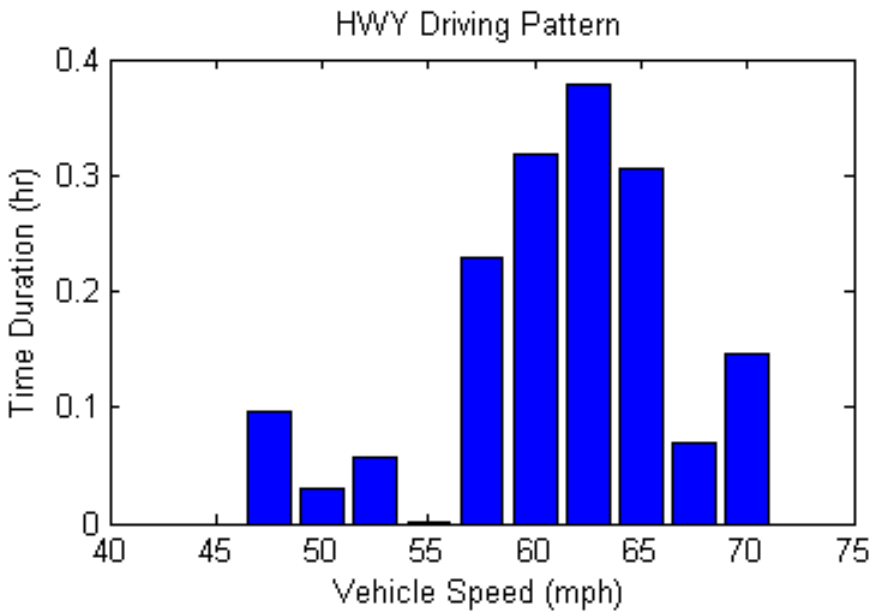

Figure 3.4: GA optimal pattern for highway scenario with the lowest fuel consumption.

Two predefined drive cycles by the EPA were used as a benchmark for the determined driving patterns via the GA. Using the FTP and US06 drive cycles in Eq. (7) for comparison; Table 3.2 demonstrates the improved fuel economy for the determined driving patterns via the GA over the predefined cycles.

Table 3.2: Fuel consumptions comparison for GA determined driving patterns and EPA drive cycles.

	Distance (mi)	Avg. Spd. (mph)	MPG
GA city	10	38.32	20.35
GA hwy	100	62.18	25.62
FTP	11.04	21.21	16.22
US06	8.01	48.37	23.63

3.5 Distance Sensitivity

Distance sensitivity studies were done to see the effect of distances selected for both the city and the highway scenarios used in the model. Figure 3.5 shows an average fuel consumption of 19.4 MPG with 3.8% variation for distances between d = 5 to 20 miles for the city scenario. The highway driving scenario shows an average mpg of 25.5 mpg with a slight decrease of 1.2% between the distance range of d = 50 to 200 miles (see Figure 3.6). It is safe to say that the distance used for both the city and highway scenarios in the model (10 and 100 mi.) have minimal impact on the results.

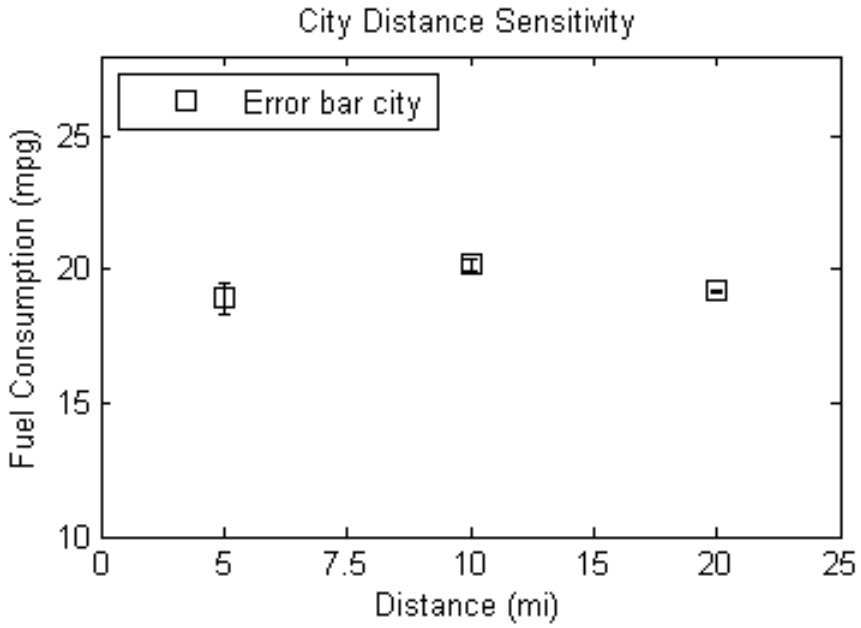

Figure 3.5: Distance traveled effect on vehicle fuel economy for the city scenario.

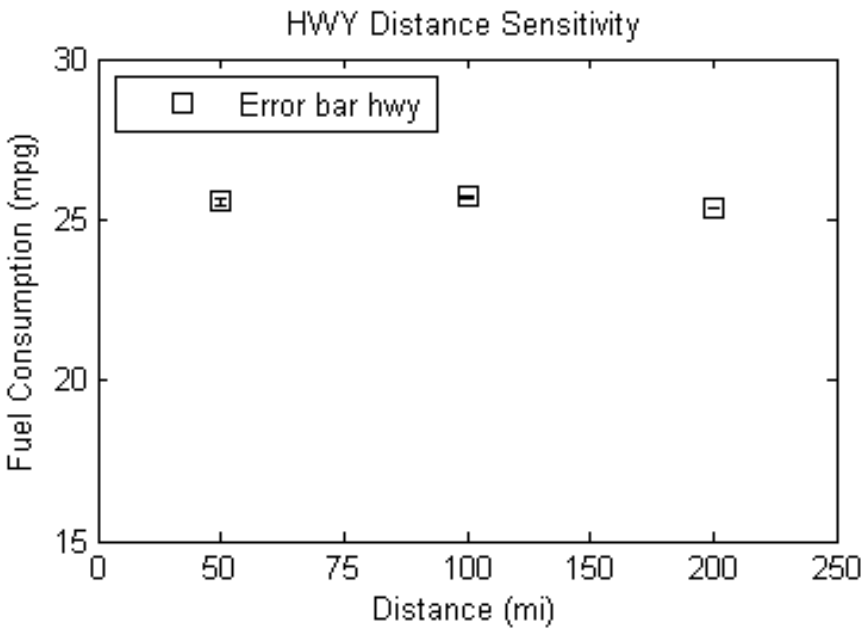

Figure 3.6: Distance traveled effect on vehicle fuel economy for the highway scenario.

For the EcoCAR2 competition, the team will be scored on how much petroleum energy is consumed by the vehicle when travelling the required distance of 200 miles. While the competition requires that the vehicle has to be able to travel a distance of 200 miles, the mass of liquid fuel consumed during the trip of approximately 100 miles will be calculated for scoring. The figures above show the robustness of the optimal driving patterns determined using a GA optimization method up to 200 miles for the highway scenario.

3.6 Conclusion

This chapter demonstrated a model-based approach to determine the optimal driving patterns with the lowest fuel consumption for both the city and the highway scenarios via a GA

optimization method. By utilizing experimental engine data as input parameters, a numerical model was developed to determine the optimal driving patterns for the two scenarios. An optimal driving pattern is a collection of driving times and driving speeds used to cover a given distance with the least amount of fuel. For the city driving scenario, driving speeds near 35 and 45 mph were found to yield the lowest amount of fuel consumption; around 60 mph for the highway driving scenario. Remaining around these speeds means that drivers minimize the driving period when the ICE would perform at inefficient levels; the period of lower speeds when an engine's torque and horsepower is low, but fuel requirement thresholds must be maintained.

These normative driving patterns provide key information on how long one should drive at a given speed to attain the best fuel economy and can now serve as the axioms for an adaptive control strategy. They also allow us to determine how best to adapt the power characteristics of the electric traction motor, ICE and the ESS, the three components regulated by an adaptive control strategy in chapter 4.

Chapter 4
Adaptive Control Strategy Development (Part 2)

This chapter introduces an adaptive control strategy for a series PHEV which incorporates the complexity of human driving behavior. The optimal driving patterns determined in Chapter 3 provide a piece of the puzzle to develop the adaptive control strategy. By taking these known driving patterns for the conventional ICE vehicle along with the inefficiency of the electric traction motor at high speed, an intelligent EMS can be derived to improve vehicle efficiency. With this information, an adaptive control strategy is derived to adjust the energy distribution between the ICE and the ESS for a series PHEV. This control strategy is modeled and integrated in the Advanced Vehicle Simulator (ADVISOR) software using the Simulink/MATLAB platform. The results of the vehicle performance and efficiency for the adaptive control strategy will be discussed in this chapter.

Due to the highly complex system design and vehicle architecture of hybrid vehicles, sophisticated EMS are required to optimize the vehicle's performance. As part of the EcoCAR2 competition, NCSU students are challenged to build the next generation of hybrid

vehicle. These hybrid vehicles must be designed to reduce fuel consumption, reduce tailpipe emissions and maintain consumer acceptability in the area of performance, utility and safety. Given this specification, the team was provided with a 2013 Chevrolet Malibu to use as the integration platform for the new hybrid design vehicle. The 2013 Chevrolet Malibu vehicle parameters are used in ADVISOR to investigate the performance of the adaptive control strategy relating to the vehicle performance and efficiency. Table 4.1 shows the 2013 Malibu parameters along with the components used for modeling the series PHEV. The ESS has a nominal of 292 V rated at 16.2 kW-hr provided by A123 Systems. The 97 kW electric traction motor is manufactured by Magna. A 60 kW generator by TM4 Electrodynamics is directly coupled to a 50 kW Kubota diesel ICE.

Table 4.1: 2013 Chevrolet vehicle data and components used in ADVISOR simulations.

Vehicle	2013 Chevrolet Malibu
Drag coef.	0.295
Frontal area	0.295 m^2
Rolling resistance coef.	0.009
Hybrid configuration	Series PHEV
Vehicle mass	1800 kg
ICE	1.5 L Diesel 50 kW
Generator	TM4 Elecrtodynamic 60kW
Traction Motor	Magna E-Drive 97 kW
Energy Storage System	A123 6x15s3p Prismatic cells
	Nom. Voltage 292V, 16.2kW-hr

Based on the selected components and parameters in Table 4.1, the DOH for the vehicle can be calculated as follow:

$$DOH = \frac{P_{EM}}{P_{EM} + P_{ICE}} = \frac{97\ kW}{97\ kW + 50kW} = 0.659$$

While the DOH of the NCSU series PHEV is marginally larger than 0.65, it is within reasonable limit to provide the necessary power required for vehicle propulsion.

4.1 Control Strategy

The concept of a control strategy is to facilitate the communication pathway and the energy available onboard of the vehicle for best performance and efficiency. For this research, the term control strategy is used to describe the power distribution between the ESS and the ICE. The goal is to balance the ESS electrical power demand and the ICE to achieve the most efficient energy combination to maintain vehicle performance and drivability.

The control strategy uses the optimal driving patterns determined offline via a GA to manage the energy distribution in a PHEV. Knowing the driving patterns that consume the least amount of fuel for the conventional ICE vehicle can provide insight for adjusting the energy distribution between the ESS and ICE. The optimal driving patterns found for the conventional ICE vehicle show that, in order to consume the least amount of fuel, the majority of the driving speed resided at relative high velocity, $v_1 = 35\,mph$ and $v_2 = 45\,mph$ for the city and $v_3 = 62.5\,mph$ for the highway driving scenario (see Figures 3.3 and 3.4). Maintaining these speeds for long durations yields the highest efficiency for

conventional ICE vehicles; however, they are not efficient driving speeds for series PHEVs due to the inefficiency of the traction motor operating at high speed.

As shown in Figure 4.1 (a), the power required for vehicle propulsion is nonlinear as vehicle speed increases. As the gradient increases, the efficiency of the traction motor decreases. Similarly, the ESS SOC gradient decreases as the vehicle speed increases in a nonlinear fashion (see Figure 4.1 (b)). Due to the inefficiency at these relatively high driving speeds caused by the large energy gradient required by the traction motor, an adaptive upper and lower bound of the SOC limit is introduced to manage the power demand between the ESS and the ICE during a drive cycle.

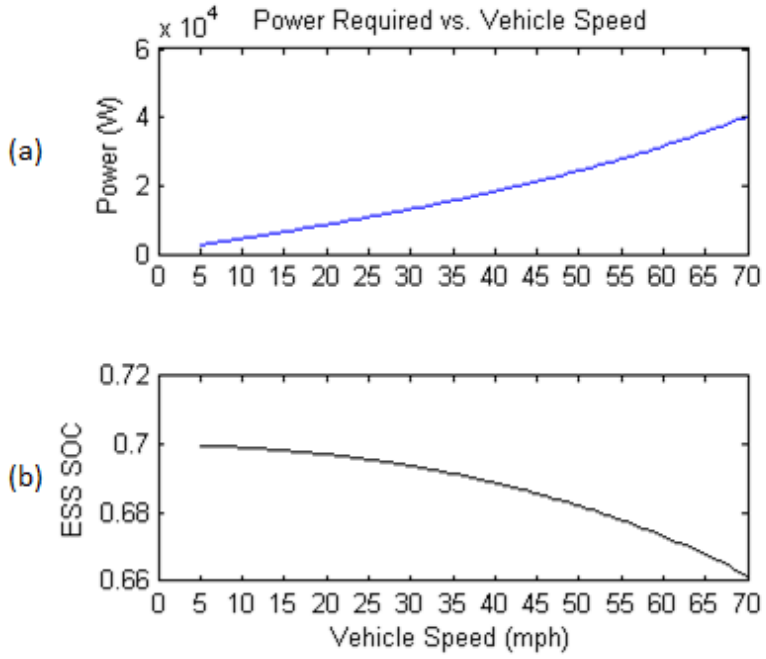

Figure 4.1: (a) Power required for traction motor vs. vehicle speed (b) ESS SOC vs. vehicle speed.

4.2 Simulink Model

This section looks at the development of the adaptive control strategy in Simulink and implementation in ADVISOR. The adaptation of the SOC upper and lower limits is a simple concept: once the vehicle speed crosses an undesired velocity condition, new upper and lower bounds are defined based on the SOC and vehicle speed, and they remain true until the condition is no longer satisfied. The new SOC bounds are constantly changing and adapting to the driving conditions. An if-then rule-based control is applied to ensure the conditions are satisfied.

Figure 4.2 illustrates a high level of the Simulink model for the adaptive control strategy. The vehicle speed is used as a primary input to facilitate the control logic for the control strategy. Two operation modes are considered: Mode 1 is when the vehicle speed is $\geq$ 45 mph and mode 2 is when the vehicle speed is $\geq$ 62.5 mph. The two outputs in Figure 4.2 (Out1 and Out2) are the upper and lower SOC limits based on the driving conditions. The switching from static upper or lower SOC limits to adaptive control limits is done using the block Switch4 as shown in Figure 4.2. When the vehicle speed is $\geq$ the set vehicle speed threshold (cs_threshold_mode1 = 45 mph), the upper and lower limits switch to the new adaptive limits contained in Subsystem_hi and Subsystem_lo, respectively. In order to force an exit when the vehicle is no longer in the adaptive control mode, a break block (Subsystem_soc_hi_break) was designed to return to the static SOC limits. The Subsystem_soc_hi_break block was designed so that the upper limit would momentarily drop

to a lower limit and force an exit due to violating the if-then conditions. A more detailed procedure of the Simulink model for the adaptive control strategy can be found in Appendix A.

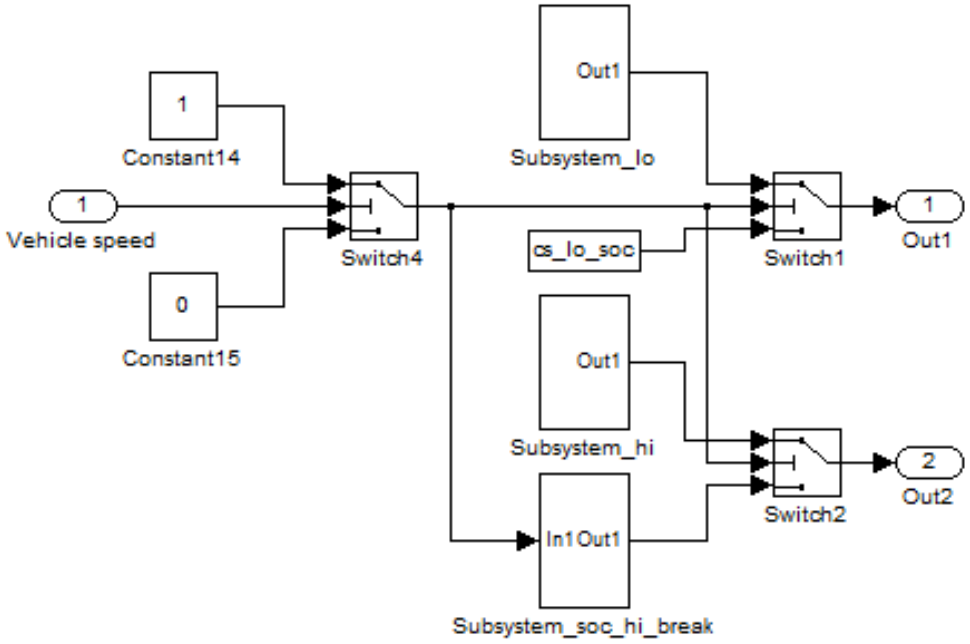

Figure 4.2: Simulink model of adaptive control strategy.

Figure 4.3 shows the logic functions of the Subsystem_lo block shown in Figure 4.2. Here the SOC information is used to define the adaptive upper and lower limits when the vehicle is in the adaptive control region. The lag controller is used to regulate the input responses from the SOC input, which defines the new upper and lower limits. Depending on the SOC, the upper and lower limits ratio is governed in the Subsystem_gain_lo block.

Moreover, the Subsystem_gain_lo also set the bandwidth parameters for mode 1 and mode 2 in the control strategy.

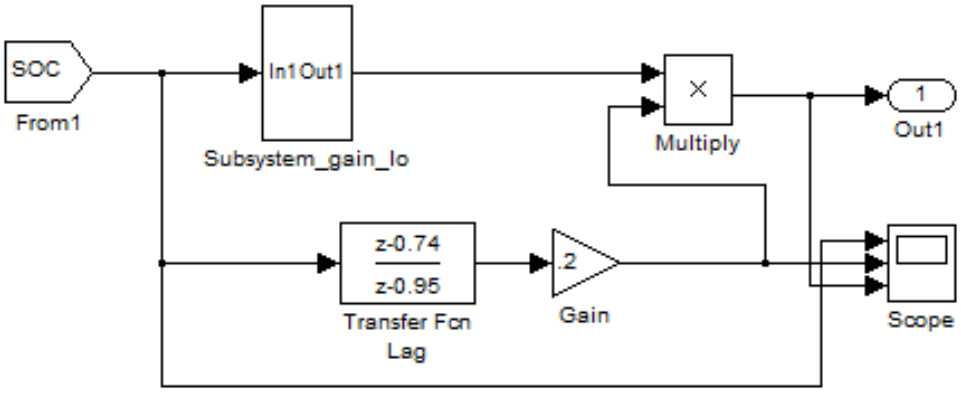

Figure 4.3: Adaptive control strategy Subsystem_lo block.

The adaptive control for the ICE active state is as follows:

- ICE is on if the velocity conditions are true (vehicle speed $\geq v_2$ *and or* v_3) and violate the lower SOC limits.
- ICE is off if the velocity conditions are true (vehicle speed $\geq v_2$ *and or* v_3) and violate the upper SOC limits.

Figure 4.4(b) illustrates a close-up of the adaptation SOC limits (upper and lower in blue and red, respectively) as the vehicle enters $v_2 = 45\,mph$ and $v_3 = 62.5\,mph$ for a US06 drive cycle. Due to the smaller power requirement for v_2 than v_3, the SOC limit bandwidth is larger within v_2 compared to v_3. The newly defined bandwidths help avoid triggering the ICE due to sudden acceleration during real driving conditions. The initial SOC

of 0.7, SOC lower limit of 0.2 and SOC upper limit of 0.8 are used in this study along with the parameters in Table 4.1. The model is built in Simulink and integrated in ADVISOR using MATLAB 2010b. Tuning the parameters of the adaptive control strategy is shown in the subsequent section.

4.3 Controller Parameter Tuning

This section examines the different parameters of the adaptive control strategy and how they affect the vehicle performance and efficiency. The aim is to tune the controller design to yield the best overall performance and maintain robustness throughout the duration of a drive cycle. Of interest is the SOC characteristic, where the linear and predictable SOC over a drive cycle is desired. The three variables of interest pertaining to the proposed adaptive control strategy are as follows: the lag controller design, bandwidth limits, and upper and lower limits ratio.

4.2.1 Lag Controller Design

A lag controller is used to define the new upper and lower limits in the adaptive control strategy. A lag controller is similar to a proportional-integral controller; it is useful for reducing the step-response steady-state tracking error and overshoot (Chow et al. 2002). Consider a continuous-time transfer function in the form of:

$$G_c(w) = K_w \left(\frac{w - w_z}{w - w_p} \right)$$

Where $G_c(w)$ is the lag compensator, K_w is the gain, w_z is the zero and w_p is the pole. With this first-order continuous-time transfer function a controller was designed and tuned to meet the desired performance for the adaptive upper and lower limits. As previously mentioned, the ability of the upper and lower limits to follow the SOC will have a significant impact on the performance of the vehicle. This section evaluates the effect of different w_z values, w_p values and K_w values on the ESS SOC over a drive cycle. Figure 4.4 illustrates the effects of different w_z values on the ESS performance over the US06 (x8) drive cycle.

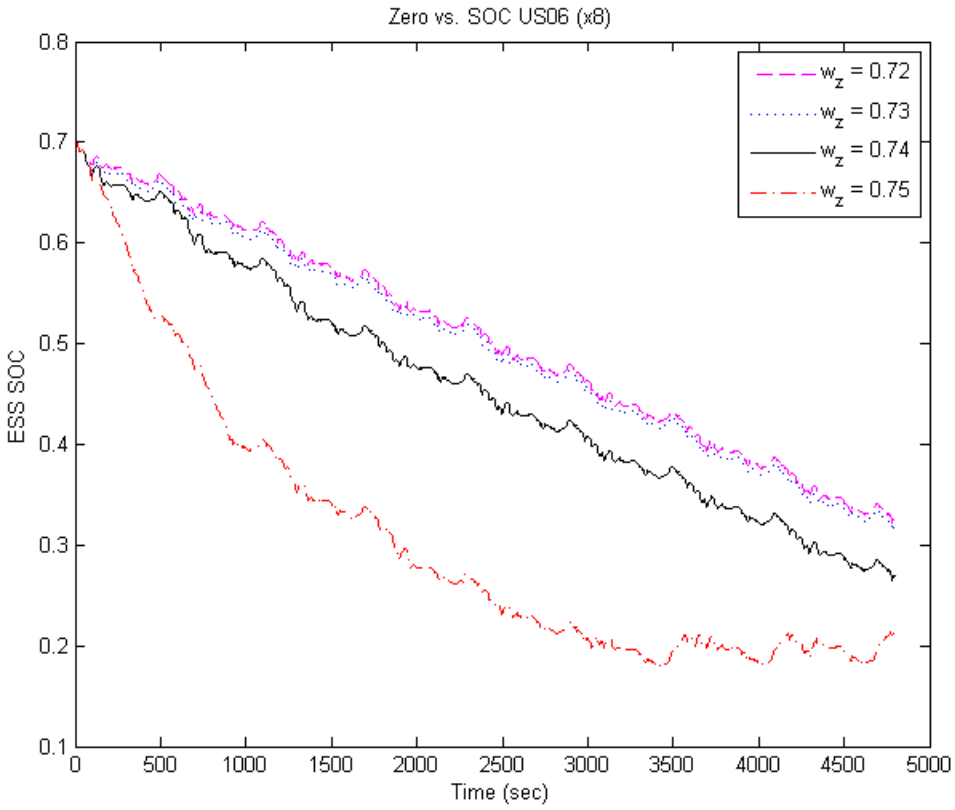

Figure 4.4: Zero effects on ESS performance with w_p = 0.95 and K_w = 0.2.

For w_p = 0.95 and K_w = 0.2, Figure 5.1 shows that for a zero value of w_z = 0.75, the SOC decreases rapidly, which means that the vehicle predominately relies on the ESS to power the vehicle. This high discharge rate in turn increases the thermal generation from the ESS which increases the likelihood of a catastrophic failure. While the zero values of w_z = 0.72 and 0.73 exhibit a linear relationship over the drive cycle, they rely more on the power of the ICE to provide the power required to drive the vehicle. This will increase the amount of fuel consumed over the drive cycle, which is not efficient. A zero value of w_z = 0.74 is well balanced between power distribution and vehicle performance, where a linear relationship is seen with additional utilization of the ESS to balance the power demand from the ICE.

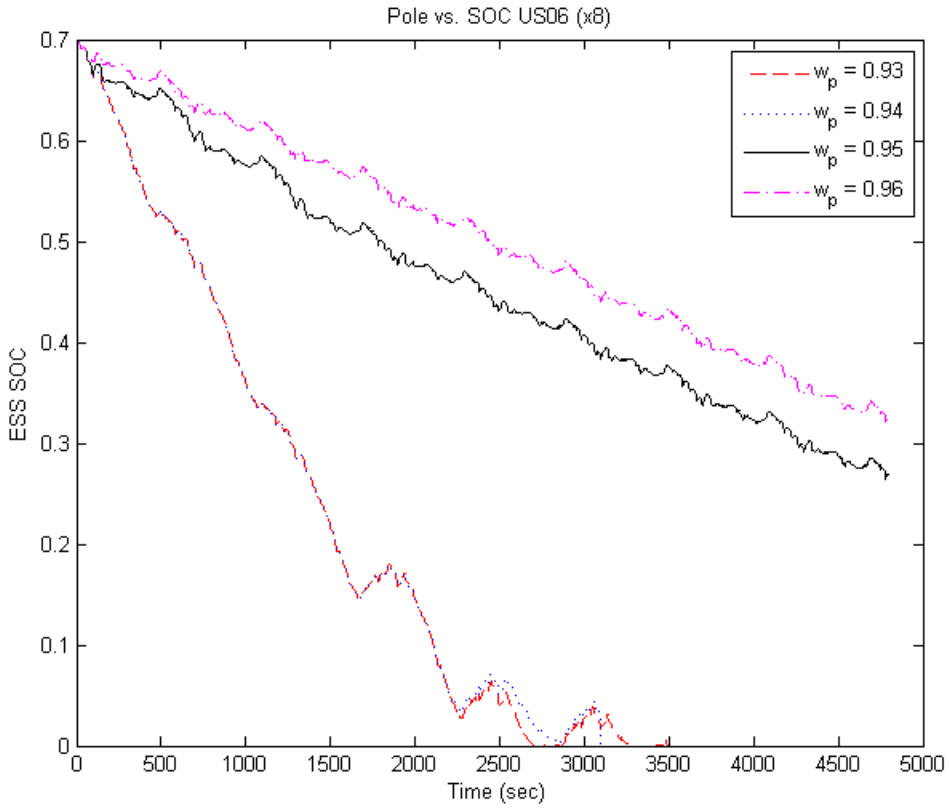

Figure 4.5: Pole effects on ESS performance with w_z= 0.74 and K_w = 0.2.

Figure 4.5 shows the response for different pole values versus the SOC characteristics for the US06 (x8) drive cycle. For w_z= 0.74 and K_w = 0.2, the pole values of w_p = 0.93 and 0.94 drive the SOC down extremely lower SOC limit near zero, this could lead to degradation of the ESS making the power unusable. On the other hand, w_p = 0.96 would require the ICE to stay active more frequently, resulting in higher fuel consumption, which is less efficient. A pole value of w_p = 0.95 is selected based on the desired performance and

ability to follow the power demand without drastically depleting the ESS during a drive cycle.

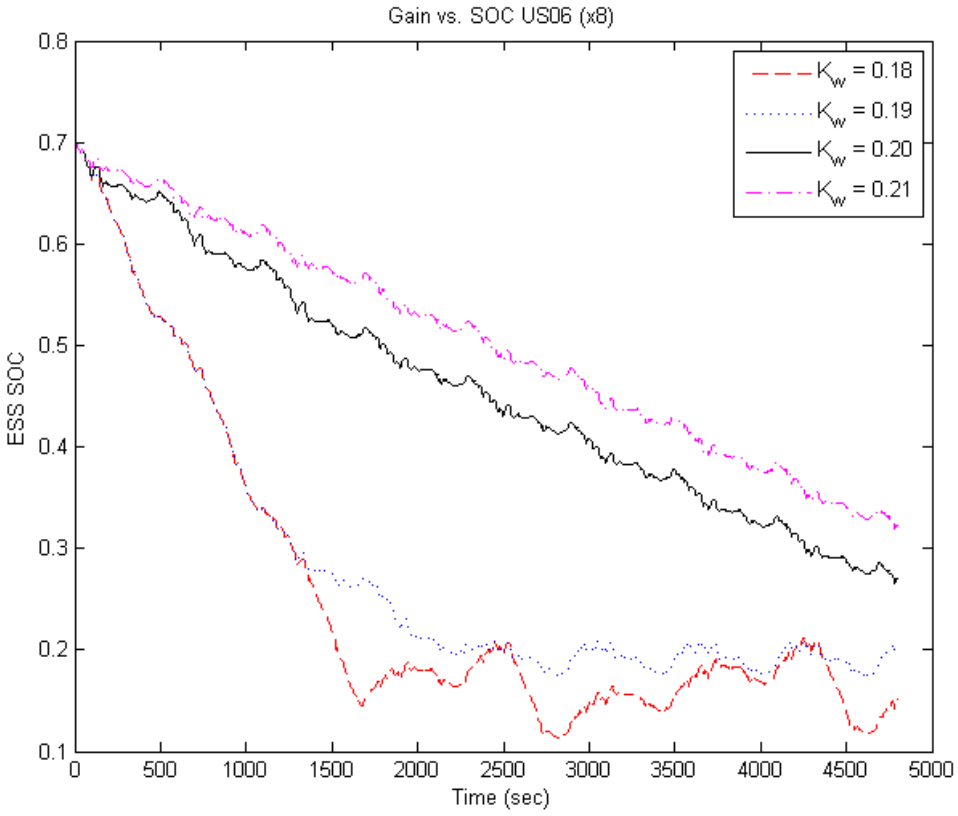

Figure 4.6: Gain parameter for the lag controller with w_z= 0.74 and w_p = 0.95.

Similar to the zero and pole, the different gain value of the lag controller can impact the characteristic of the lag controller. Figure 4.6 illustrates the effect of different gain values (K_w = 0.18 to 0.21) on the ESS SOC characteristics. A gain value of K_w = 0.2 is selected for

the lag controller as it exhibits the best performance and meets the design target. The final design parameter of the lag controller takes the form of:

$$G_c(w) = 0.2\left(\frac{w - 0.74}{w - 0.95}\right)$$

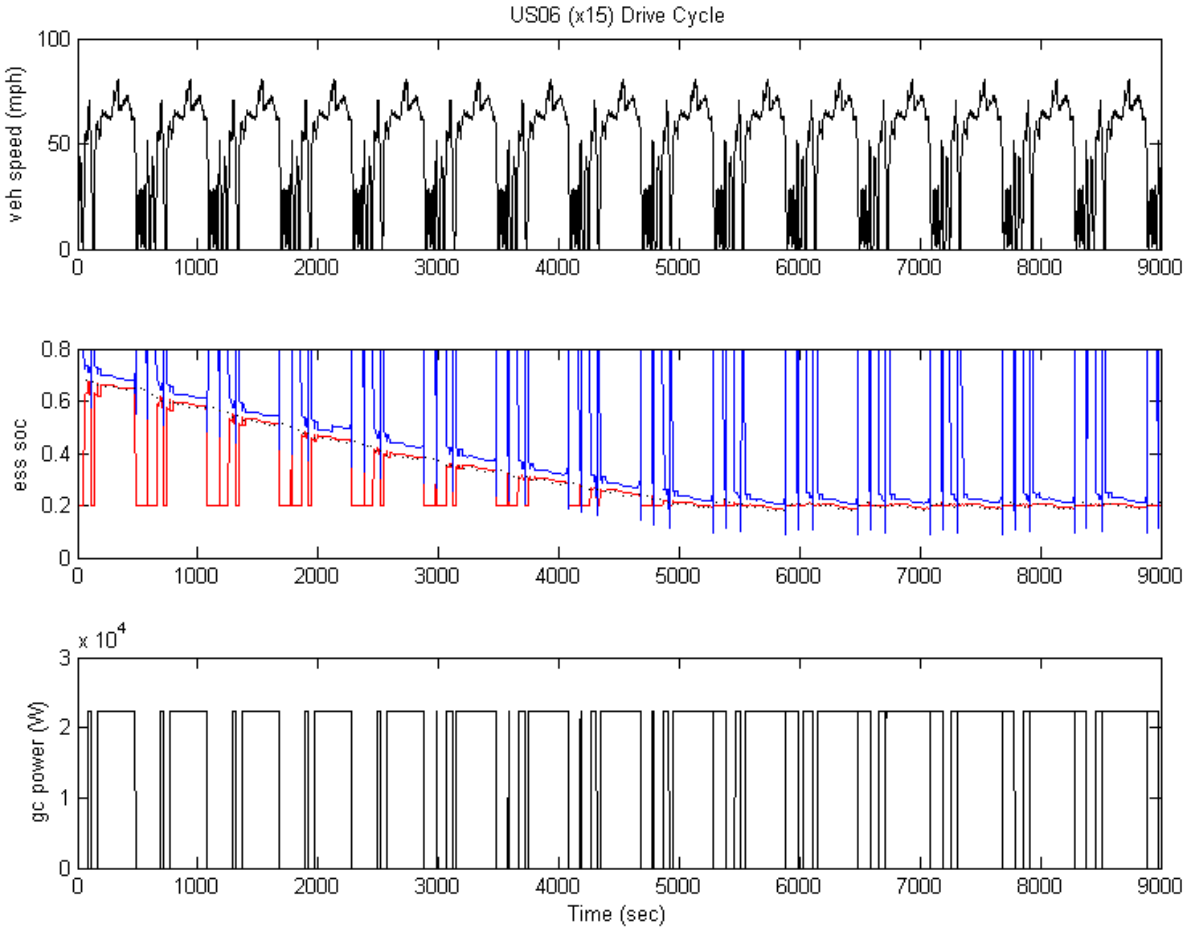

Figure 4.7: US06 (x15) drive cycle with lag controller as designed.

The final design of the lag controller exhibits good performance and adaptability for a series PHEV. Figure 4.7 shows the performance and adaptability of the final lag controller design over the US06 (x15) drive cycle. As can be seen in Figure 4.7 (b) the upper and lower SOC limits follows the SOC closely to ensure the desirable performance over the drive cycle. While the upper and lower SOC limits effect the ESS characteristics, the bandwidth values of these limits can impact the adaptive controller performance significantly.

4.2.2 Bandwidth Value

The bandwidth values play a critical role in the performance of the adaptive controller. If the values are too large or too small, the vehicle will operate in a non-efficient regime. As previously, the bandwidths are designed to take on different values depending on the driving conditions. In this research, two driving modes are defined in the control strategy (mode 1 and mode 2). For mode 1, the vehicle is operating at a lower speed, $v \geq 45\ mph$, and mode 2 at higher vehicle speed $v \geq 62.6\ mph$. Mode 2 takes on a smaller bandwidth than mode 1 in order to compensate for the larger power demand from the electric traction motor. The smaller bandwidth value for mode 2 would force the ICE to become active more frequently than in mode 1. The goal of this section is to select the best combination of bandwidths for modes 1 and mode 2 to meet the desirable performance and efficiency. A bandwidth range of 0.05 to 0.2 for mode 1 and bandwidth range of 0.02 to 0.2 for mode 2 will be examined.

Table 4.2: Bandwidth parameter for driving modes 1 and 2 effect on fuel economy.

	Bandwidth	US06 (x8) - MPG	US06 (x10) - MPG	US06 (x15) - MPG
Mode 1	0.05			
Mode 2	0.02	44.2	44.2	40.2
Mode 2	0.05	44.2	44.2	40.2
Mode 2	0.08	44.2	44.2	40.2
Mode 1	0.1			
Mode 2	0.02	46.1	46.6	40.2
Mode 2	0.05	46.1	46.6	40.2
Mode 2	0.08	47.7	46.7	40.2
Mode 1	0.15			
Mode 2	0.02	47.8	44.7	40.2
Mode 2	0.05	47.8	44.7	40.2
Mode 2	0.08	49.1	44.7	40.2
Mode 1	0.2			
Mode 2	0.1	48.8	44.6	40.2
Mode 2	0.15	48.7	44.6	40.2
Mode 2	0.2	48.7	44.6	40.2

Table 4.2 shows the fuel economy for different bandwidth values for the US06 (x8 to x15) drive cycle extracted from ADVISOR. As illustrated in Table 4.2, when mode 1 bandwidth is less than 0.1 lower fuel economy is seen. Similarly, when the bandwidth is greater than 0.2, fuel economy begins to decrease. This allows us to refocus on the region of interest for the mode 1 bandwidth range of 0.1 to 0.15. The mode 1 bandwidth of 0.15 and mode 2 bandwidth of 0.08 yielded the highest fuel economy with a steady and linear performance of the SOC. The combinations of mode 1 and mode 2 bandwidths (highlighted

in Table 4.2) that exhibit the best fuel economy are selected to examine the SOC characteristics as shown in Figure 4.8.

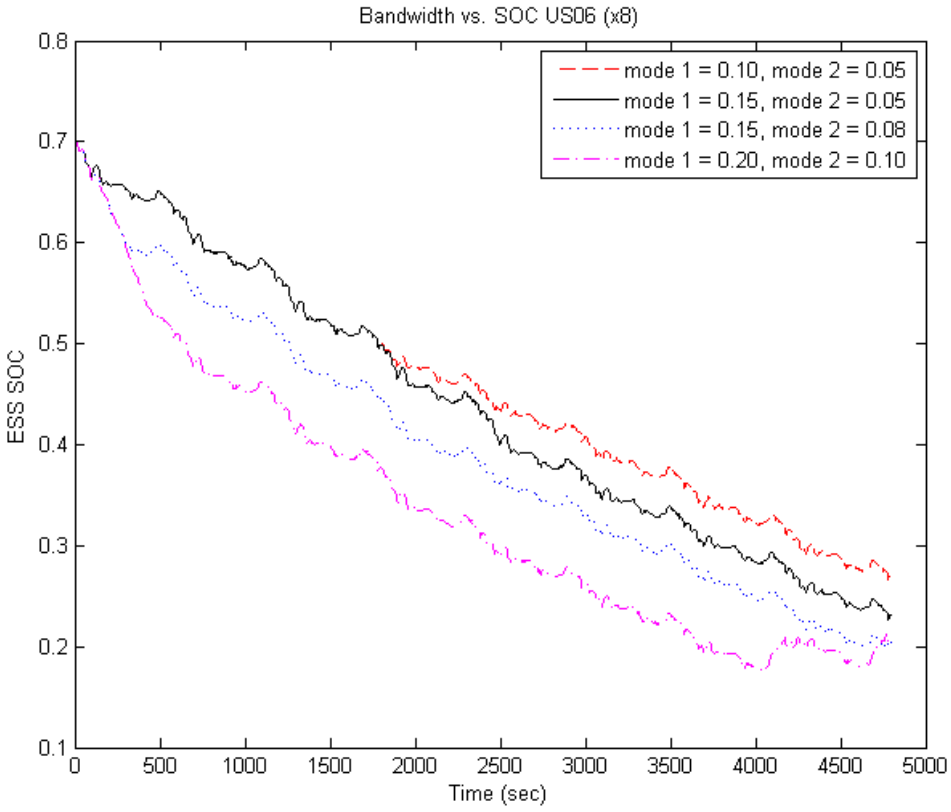

Figure 4.8: SOC performance for four selected bandwidth combinations.

As shown in Figure 4.8, setting mode 1 = 0.10 and mode 2 = 0.05 would require the ICE to stay active longer and hence lower fuel economy. When mode 1 = 0.15 and mode 2 = 0.05 they exhibit similar discharge rate as mode 1 = 0.15 and mode 2 = 0.08. For mode 1 = 0.2 and mode 2 = 0.1, the fuel economy begins to decrease, because it relies more on the ESS during the first 4,000 sec. While mode 1 = 0.15 and mode 2 =0.08 has a higher MPG (49.1)

compared to the 47.8 MPG for mode 1 = 0.15 and mode 2 = 0.05, the sharp decrease at the start of the drive cycle corresponds to a high ESS discharge rate, which is undesirable. In order to preserve the desired design performance, mode 1 = 0.15 and mode 2 = 0.05 were selected as the final the bandwidth values.

4.2.3 Upper and Lower Limits Ratio

The upper and lower (U/L) limits' ratio responses to the adaptive control strategy are examined in this section. The selected U/L ratio reflects the desired criteria to attain good performance for a series PHEV based on the design combinations of the lag controller and bandwidth values in sections 4.2.1.and 4.2.2. Two U/L limit ratio strategies are considered: a) fixed ratio of 50 percent upper and 50 percent lower; b) variable ratio with the inverse relationship (1 - SOC) of the SOC. The fixed U/L ratio (0.5) allows for a constant U/L during the drive cycle, which does not take into account the changing state of the SOC. The variable U/L ratio, on the other hand, would allow compensation for the changing SOC over a drive cycle. For instance, when the SOC = 0.7 would give a U/L ratio of 0.3, if the SOC = 0.3 the U/L ratio is 0.7. This configuration allows for more energy to be drawn from the ESS when the ESS is at a higher SOC and, as the SOC decreases, lowers the amount energy that is drawn from the ESS. This helps facilitate the ICE staying active longer as the SOC approaches the lower SOC limit. Figure 5.6 illustrates the fixed U/L ratio for a close-up section of the US06 drive cycle (in blue) and the variable U/L ratio (in red).

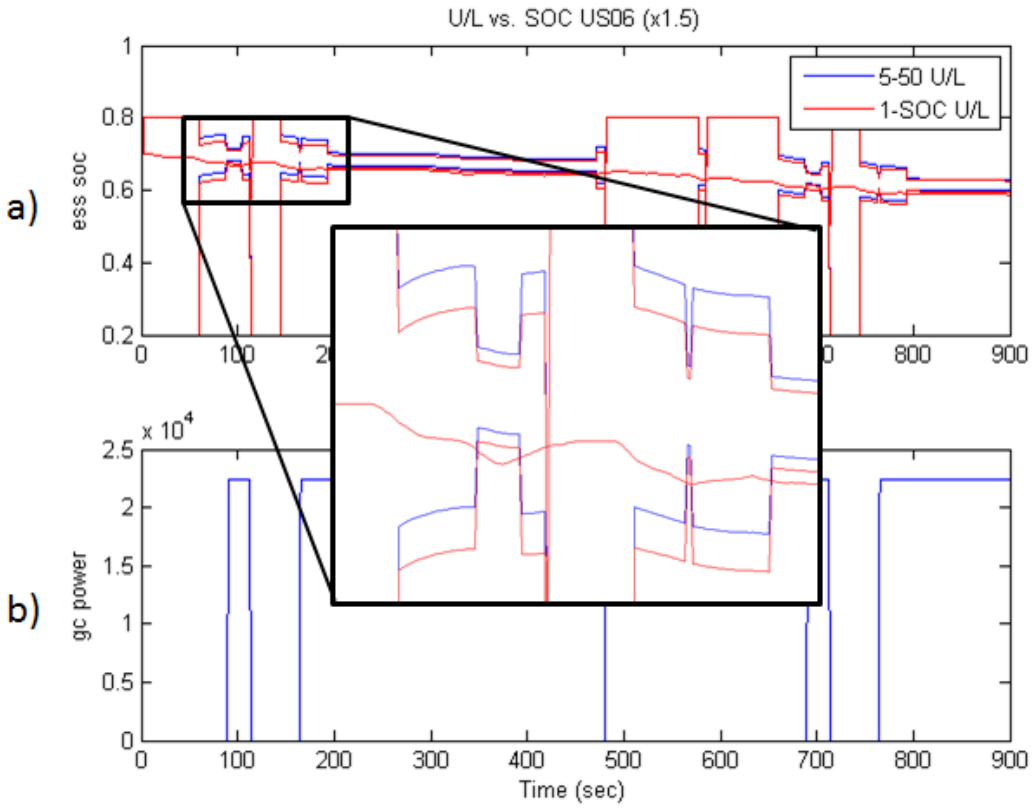

Figure 4.9: Upper and lower limits ratio effect on SOC for US06 (x1.5) drive cycle.

As shown in Figure 4.9(a) in red, the U/L ratio variable as the vehicle enters the newly defined upper and lower limits, 70 percent of bandwidth belongs to the lower limit and 30 percent to the upper limit. The fixed U/L ratio is shown in the same graph in blue, where the distribution is 50 percent between U/L as the vehicle enters the same region. While the U/L ratios shift occurred for the two U/L ratios, little effect is seen for the current design. This is not to say that is has no effect on the performance of the system, simply that based on the selected parameters for the lag controller and bandwidth values, no significant impact is seen. With this in mind, a variable U/L ratio is selected for the control strategy to maintain

vehicle performance and efficiency. The final parameters for the adaptive control strategy are selected to meet the design criteria for good performance with the desirable ESS discharge rate as shown in Table 4.3.

Table 4.3: Final design parameters for the adaptive control strategy.

w_z	0.74
w_p	0.95
K_w	0.2
Mode 1 bandwidth	0.15
Mode 2 bandwidth	0.05
Variable U/L ratio	1-SOC

This section looked at the effects of the lag controller design, bandwidth values, and U/L limits ratio on the adaptive control strategy. The final parameter selection is based on the best combinations of lag controller, bandwidth values, and U/L ratio. While it is difficult to take all variables into account, the variables studied have been shown to be highly sensitive to the overall design goal and performance. The selected parameters exhibit good performance, stability, efficiency and linear characteristics for the design of the adaptive control strategy.

4.4 Results & Discussion

Figure 4.10(a) shows the US06 drive cycle used to evaluate the adaptive SOC upper and lower limits on ESS SOC, generator state and ESS current profile. Figure 4.10(b) shows the

SOC during the drive cycle along with a close-up section when the new bounds are imposed and when the ICE is active. The momentary drop in the soc_hi limit, forcing the exit from the adaptive control mode to the static mode, is seen in Figure 4.10 (b) (the soc_hi limit in blue). Figure 4.10(c) shows when the generator is on, which is directly coupled to the ICE. Figure 4.10(d) demonstrates the lowering of electric current profile during the drive cycle when the generator is active. Reducing the discharge rate could potentially improve the ESS performance and battery life. From a performance perspective, increasing the power capability over a wide range of SOCs will allow the vehicle to access the ESS energy over a longer period.

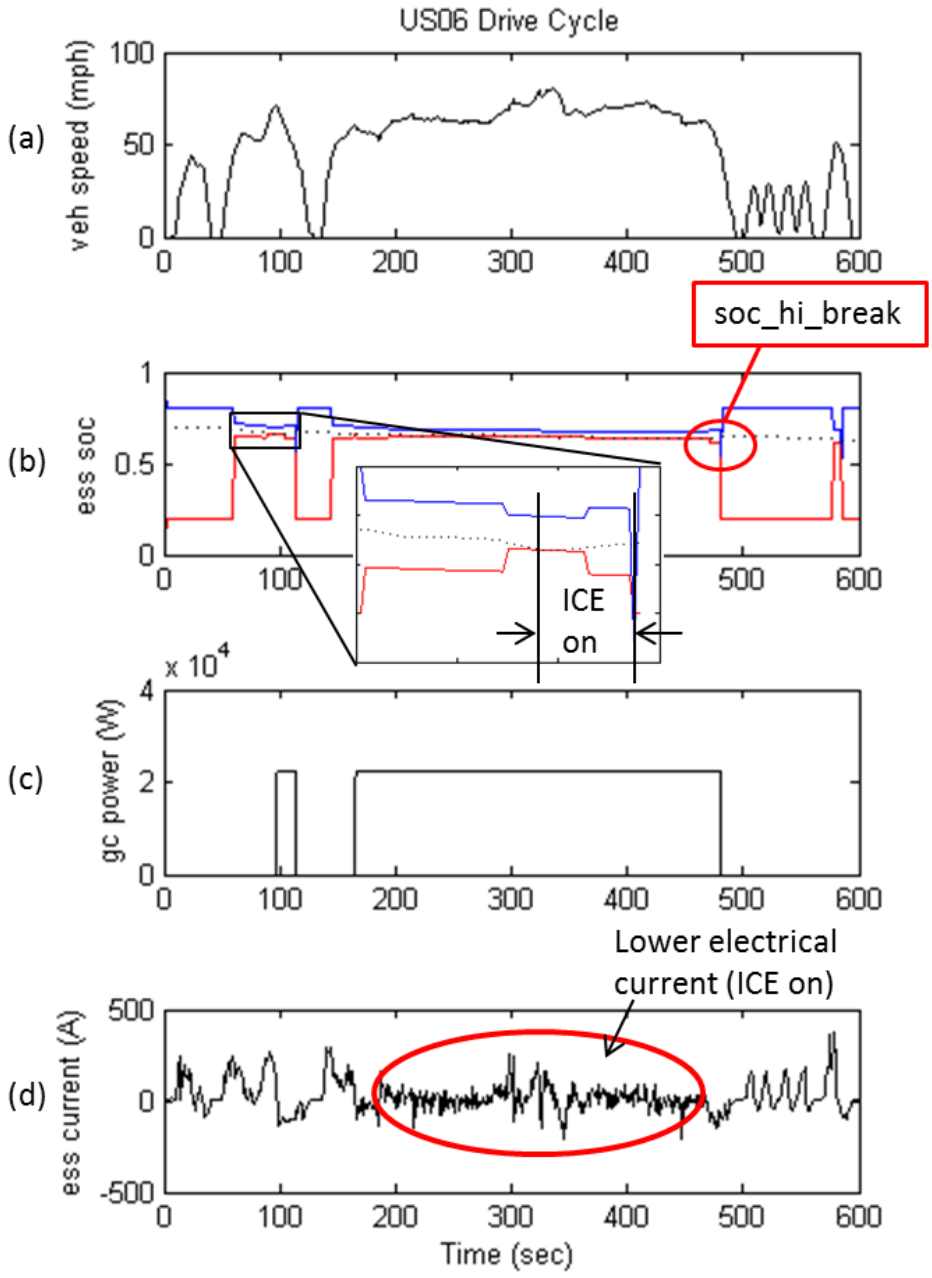

Figure 4.10: Adaptive SOC for US06 drive cycle (a) vehicle speed (b) ESS SOC with newly defined upper and lower limits in blue and red, respectively (c) generator power (d) ESS current.

Figure 4.11(a) depicts the SOC over a range of 120 miles with and without the adaptive control strategy. It is clear that when modulating the ICE (see Figure 4.11(b)), the power required by the traction motor is drawn from the ICE plus the ESS, reducing the current drawn solely from the ESS. This reduces the power drawn from the ESS when the traction motor is operating at high speeds, which is least efficient for electric motors. This will widen the usable power over a longer time duration, which can potentially improve vehicle performance.

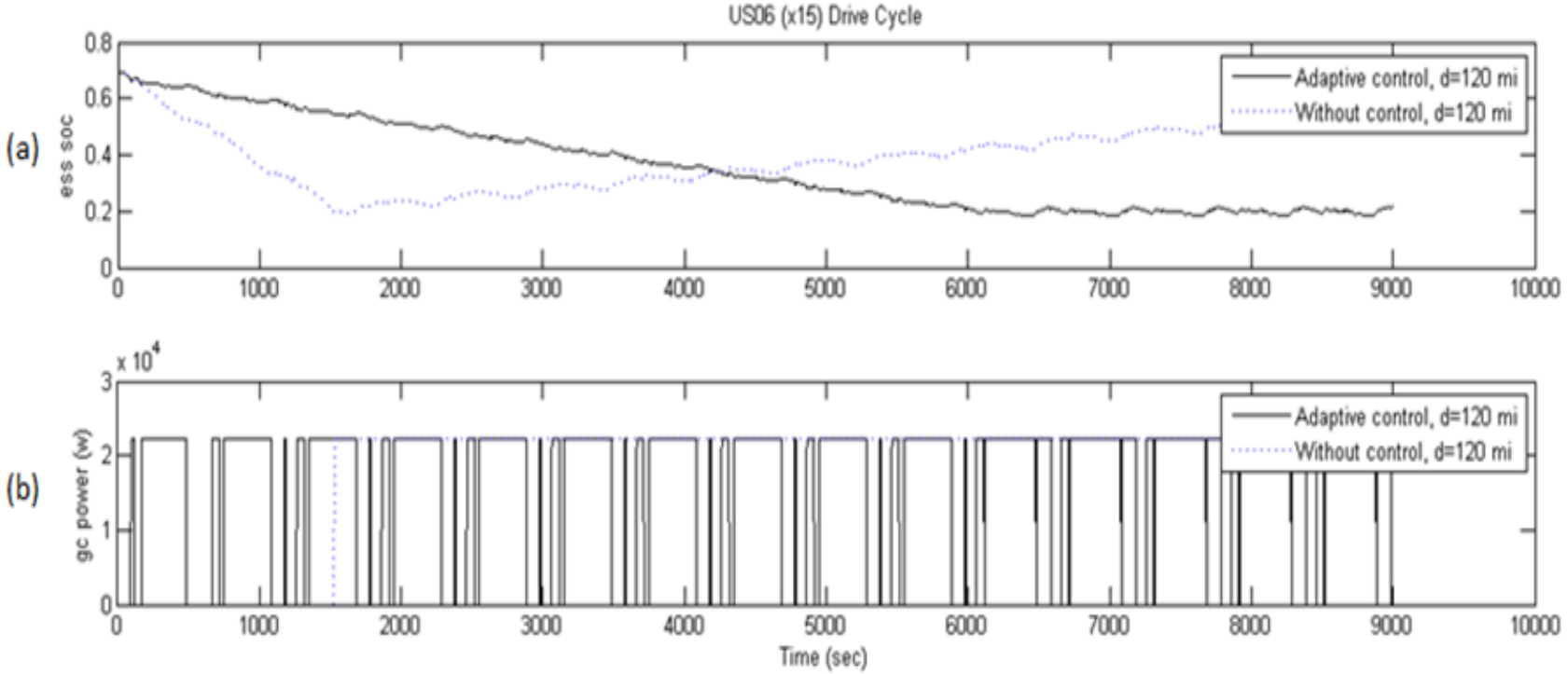

Figure 4.11: US06 (x15) drive cycle with adaptive SOC bonds and without control (a) SOC and (b) generator power.

Table 4.4 shows the fuel economy in miles per gallon (MPG) for the US06 drive cycles (x8, x10 and x15) with and without the adaptive control strategy. Controlling the upper and lower limits at the two vehicle speeds, v_2 and v_3, results in an improvement in fuel economy up to 15 percent (as shown in Table 4.4) for the US06 (x10) and (x15) drive cycles for a distance of 80 and 120 miles, respectively. On the other hand, a shorter distance (US06x8) of 64 miles shows an improvement of only 13 percent. This smaller gain in fuel economy can be explained by the larger percent of the ICE active for the distance traveled. For a shorter distance, the percent of ICE active is larger compared to a longer distance, hence smaller benefit is seen.

Table 4.4: Fuel economy with adaptive control strategy and without control strategy.

Control Strategy	Cycl.	Distance (mi)	MPG
Adaptive SOC	US06x8	64	47.8
	US06x10	80	44.7
	US06x15	120	40.2
Without control	US06x8	64	42.3
	US06x10	80	38.8
	US06x15	120	34.9

As expected, by partially activating the ICE during a drive cycle, less current is drawn from the ESS, lowering the electrical current and, in turn, reducing the amount of heat generated from the ESS. The heat generation in the ESS is through resistance heating based on the electrical current and electrical resistance given by:

$$E_g = I^2 R_e \quad (4)$$

Where $E_g$is the energy generated (W), I is the electrical current (Amp) and R_e is the electrical resistance (ohm). A complete formulation of the lumped capacitance model used for the ESS thermal analysis can be found in Appendix B.

Figure 4.10 (d) illustrates a lower current profile when the generator is on compared to when the ICE is off. Figure 4.12 shows the temperature profile for the duration of the drive cycle with the adaptive SOC upper and lower bounds compared to without adaptive control. For the US06 (x15) drive cycle, the ESS experiences a 5°C lower temperature than without the adaptive control method (see Figure 4.12).

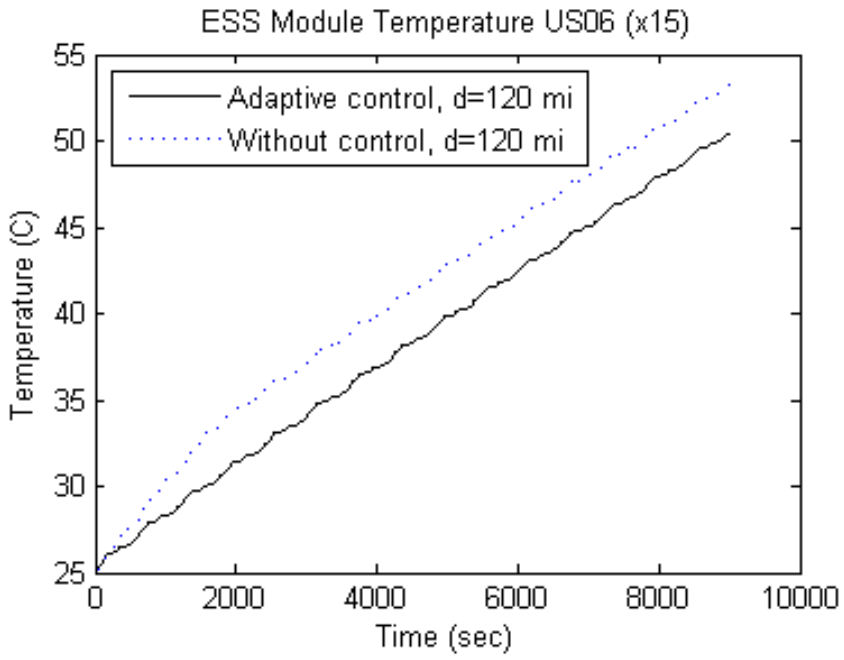

Figure 4.12: ESS temperature rise for adaptive control and without control during US06x15 drive cycle.

4.5 Conclusion

The benefits of an adaptive SOC limit for a series PHEV using determined optimal driving patterns were demonstrated in this chapter. By adjusting the upper and lower SOC limits, improved usable power capacity and a widened range of SOC over a greater distance is seen. Additionally, modulating the ICE will lower the amount of electrical current that is drawn from the ESS during a drive cycle. Having the ICE partially deactivated for a finite duration of the drive cycle will reduce the amount of fuel being consumed and potentially lower emissions. The proposed adaptive control strategy using information determined from optimal driving patterns:

- Increased fuel economy by having the ICE partially active.
- Improved vehicle performance by increasing the ESS usable power capacity over a wide range of SOC over a greater distance.
- Reduced the ESS discharge rate over a drive cycle by lowering the electrical current profile.
- Reduced the ESS heat generation and temperature profile over a drive cycle.

Chapter 5
Vehicle Communication

With the completed control strategy, this chapter looks at the vehicle communication platform for in-vehicle integration. The signals required for implementation of the adaptive control strategy for the NCSU series PHEV will be discussed in this chapter. In order to reduce the computational requirement, the adaptive control strategy uses existing signals during the development process. By taking advantage of the existing signals on the CAN bus, signals such as the ESS SOC and vehicle speed were used as inputs to the control strategy. The signals can be utilized by tapping into the CAN high and low speed buses to read and write the necessary signals to implement the adaptive control strategy. In Chapter 2, the CAN message structure and how the message is physically transmitted on the CAN bus were discussed. The use of CAN serial communication increases the efficiency and allows these linking of all communications between multiple controllers and subsystems in the vehicle. The following section describes the programming interface of CAN messages in Simulink using CAN database (dbc) files. The dbc file stored all the information required in the objects and physical layers to allow a message to transmit and receive.

The component manufacturer usually provides the dbc allowing the engineer to easily communicate and interact with the component. In some cases, only the message ID and bitwise information is available, while the control developer has to create the dbc file or manually input specific information required to have proper CAN communication. For the NCSU EcoCAR2 team, all sponsored and purchased components come with a dbc file, which makes programing more composed.

The vehicle model platform is organized in subcategories: physical signals and a supervisor model (input/output) as shown in Figure 5.1. The physical signals block organized all the inputs and outputs used in the vehicle that are utilized by the supervisory control. In order to have a robust and successful implementation of the proposed control strategy, the signals must be reliable and not overload the CAN buses. By utilize existing CAN signals for the adaptive control strategy the payload on the CAN buses can be reduced.

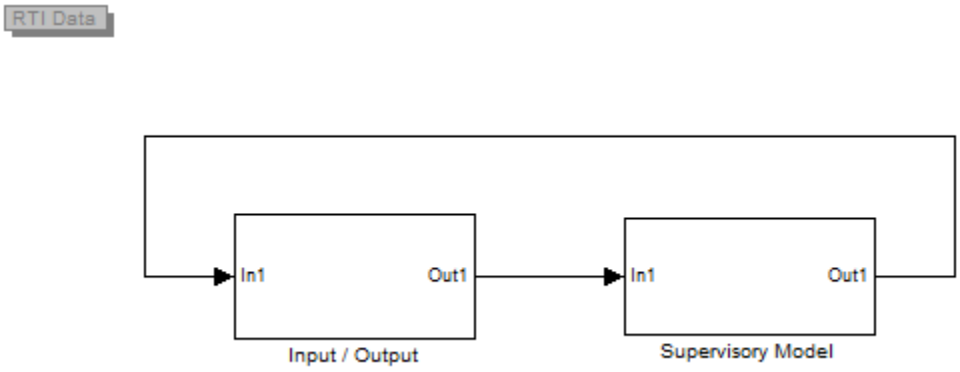

Figure 5.1: Vehicle model with input, output and supervisory controller.

While the majority of the communication within the vehicle is through CAN, analog and digital signals are also used. For safety-critical components such as the accelerator pedal and throttle position signals, hard wiring of analog and digital signals is used instead of CAN. Control signals such as the hardware wake for the ESS and the electric drive motor, digital lines are utilized. The main communication of these components is through CAN serial communication due to the large amount of data required. In the subsequent section, the details of receive and transmit CAN messages required by the adaptive control strategy are considered. Of interest are the two keys signals used by the adaptive control strategy (the vehicle speed and ESS SOC).

5.1 Creating CAN message in Simulink

This section goes into detail of creating CAN messages to be transmitted and received on the high speed CAN bus. This is important because the adaptive control strategy utilizes information from the CAN to generate information to be broadcasted on the bus. The first step in creating CAN messages is defining the CAN environment. The CAN controller can be configured to utilize the dbc file to define the signal definition in dSPACE through MATLAB/Simulink (A detailed CAN configuration setup for dSPACE in MATLAB/Simulink with dbc files can be found in Appendix C).

Figure 5.2 shows the Simulink model of the CAN messages received and transmitted from the Battery Control Module (BCM). When using the dbc file, the signal definitions are defined for all messages for a single message ID on the bus. As seen in Figure 5.2, there are

numerous messages for a single BCM_status1 CAN message. For the adaptive control, the message of interest from the BCM is the battery SOC is highlighted in a red rectangle in Figure 5.2. The ability to access the SOC state is imperative because it allows the control strategy to utilize this information when the vehicle is operating.

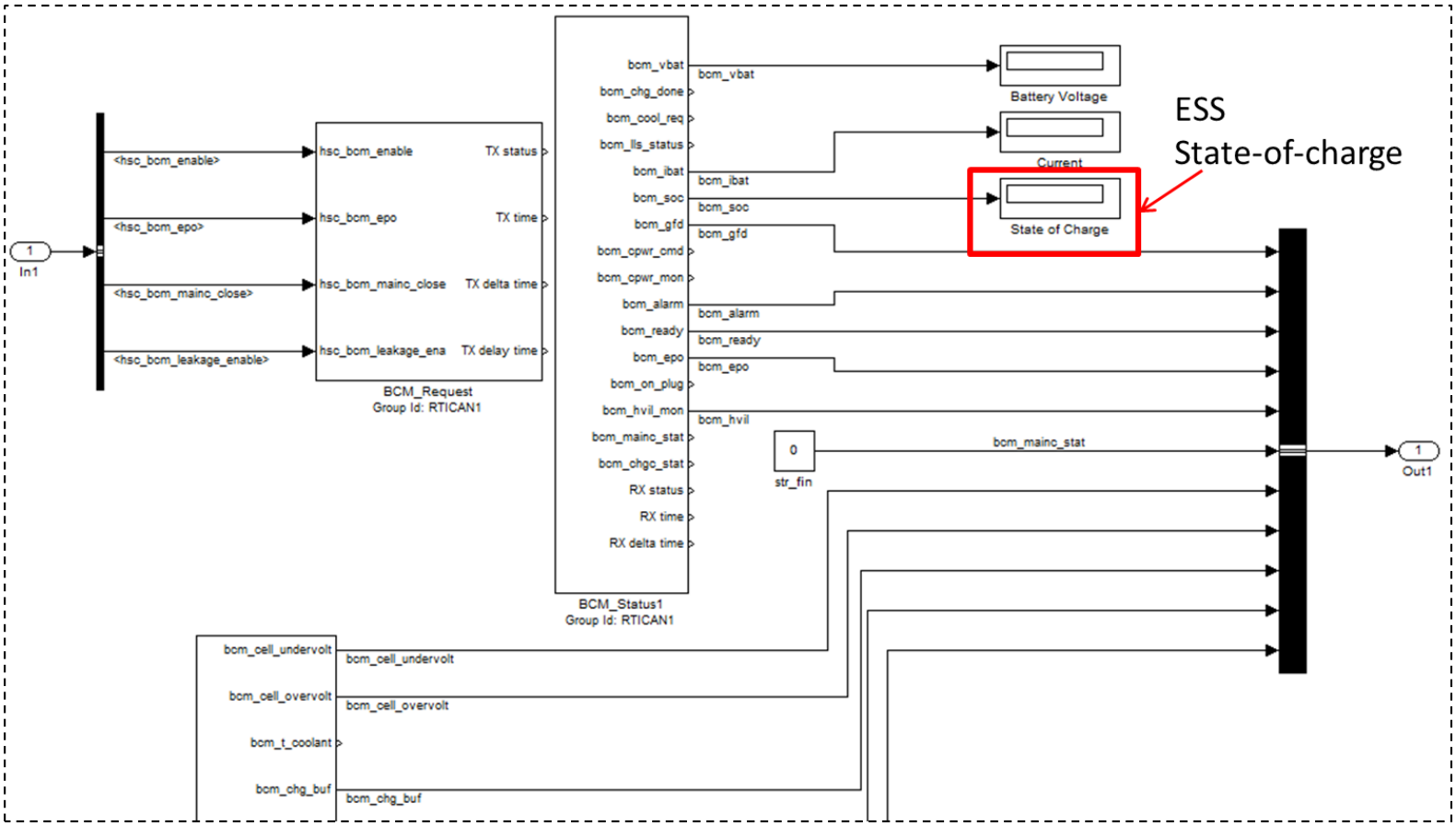

Figure 5.2: ESS state-of-charge from the BCM on the CAN bus in Simulink.

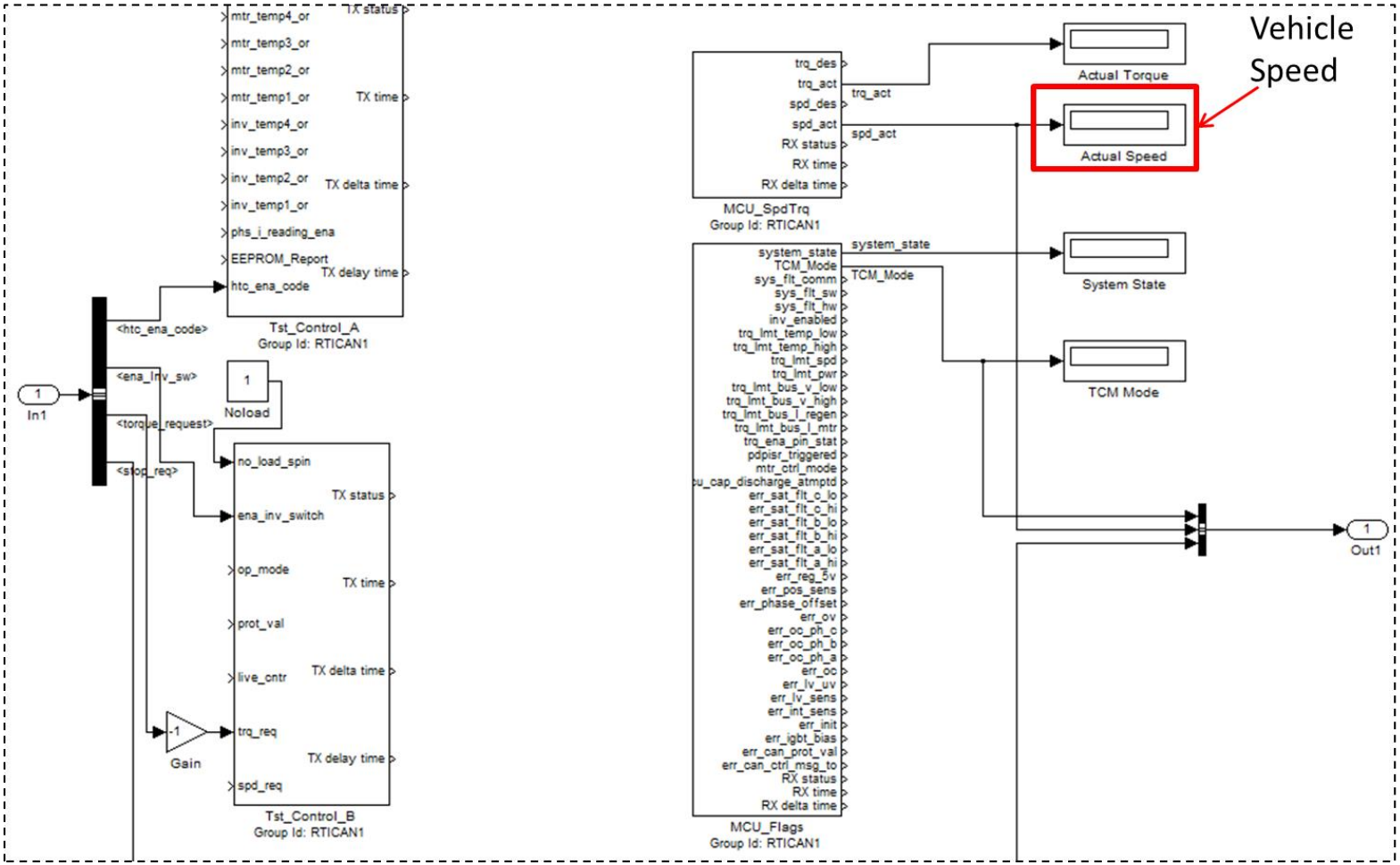

Figure 5.3: Vehicle speed from electric drive motor on the CAN bus in Simulink.

Similarly, for the electric drive motor, the information of interest (vehicle_speed) can be found on the CAN bus. The electric drive motor provides the vehicle speed for input to the adaptive control strategy, which can be extracted as shown in the red rectangular box in Figure 5.3. The vehicle speed is the other variable utilized by the control strategy to enable the desirable adaptive upper and lower limits. These two signals are used to enable different the control modes for the adaptive control strategy as described in Chapter 4.

Summary

This chapter examined the CAN messages broadcasted on the vehicle CAN buses used by the adaptive control strategy. Additionally, the process of creating and integrating CAN communication protocol for control strategies in a series PHEV was discussed. Moreover, CAN communication is important because it allows for a large amount of data to be transmitted on the CAN bus with minimum wire requirement. This enables new controls development—such as an adaptive control strategy—to be integrated with the existing vehicle at little to no additional computational expense.

Chapter 6
Concluding Remarks

An adaptive control EMS for series PHEVs was demonstrated in this research using optimal driving patterns determined via a GA to improve fuel economy and vehicle efficiency. A numerical model was developed to arrive at the optimal driving patterns for two scenarios (city and highway) utilizing a GA, which serves as design criteria for the adaptive control strategy. The determined driving patterns were used to develop an adaptive control strategy by adjusting the upper and lower SOC limits based on the driving conditions for a series PHEV. Integration of the new control strategy by utilizing existing CAN signals already available on the vehicle's CAN buses can reduce computational expenses. The proposed adaptive control strategy using information determined from optimal driving patterns:

- Improved fuel economy for a series PHEV.
- Improved in vehicle performance by increasing the ESS usable power capacity over a wide range of SOC over a greater distance.
- Reduced the ESS discharge rate over a drive cycle by lowering the electrical current profile.
- Reduced the ESS heat and temperature profile over a drive cycle

6.1 Future Work

To further understand the behaviors and performance of the adaptive control strategy for series PHEVs, a few topics of interest have been identified: (a) In-vehicle testing to validate the design and simulations of the adaptive control strategy. (b) Optimizing the ESS performance with the information from the optimal driving patterns that were determined. (c) Optimizing the vehicle performance through component sizing for PHEVs using information from the adaptive control strategy. (d) Improvement in driving mode prediction in real-time to advance the adaptive control strategy. (e) Explore new ways to adapt the adaptive control strategy to other hybrid vehicle powertrain configurations. (f) Vehicle-to-vehicle communication at a network level to improve vehicle efficiency.

REFERENCES

1. A123 Systems. 2011. “HPPC Results—Gen 1.5 20Ah Prismatic Cell.”
2. ADVISOR 2002. National Renewable Energy Laboratory.
3. Anderson, C., and Pettit, E. 1995. “The Effects of APU on the Design of Hybrid Control Strategies for Hybrid Electric Vehicles,” SAE Technical Paper. PN 950493.
4. Barsali, S., Miulli, C. and Possenti, A. 2004. “A Control Strategy to Minimize Fuel Consumption of Series Hybrid Electric Vehicles.” *IEEE*. doi:10.1109/TEC.2003.821862.
5. Bianchi, Domenico, Rolando, Luciano, et al. 2010. “A Rule-Based Strategy for a Series/Parallel Hybrid Electric Vehicle: An Approach Based on Dynaimc Programing.” *ASME* Dym. Sys. Control Conf. doi: 10.1115/DSCC2010-4233.
6. Bosch, Robert GmbH. 2010. *Automotive Handbook*. Bentley Publishers. ISBN-13: 978-1119975564.
7. Bosch, Robert GmbH. 1991. “CAN Specification.” Version 2.0.
8. Capriglione, Domenico, Consolatina Liguori, et al. 2003. “On-Line Sensor Fault Detection, Isolation and Accommodation in Automotive Engines.” *IEEE*. doi: 10.1109/TIM.2003.815994.
9. Choy, Min, and Srinivasan, Dipti, 2006. “Neural Networks for Continuous Online Learning and Control.” *IEEE*. doi: 10.1109/TNN.2006.881710.
10. Chiou, J. S., and M.-T Liu. 2009. “Using Fuzzy Logic Controller and Evolutionary Genetic Algorithm for Automotive active suspension system.” *International Journal of Automotive Technology* 10(6): 703-710. doi: 10.1007/s12239−009−0083−4.

11. Chow, H. Joe, Dean K. Frederick, and Nicolas W. Chbat. 2002. *Discrete-Time Control Problems Using MATLAB*. CL Engineering; 1st ED. ISBN-10: 0534384773.
12. Deb, Kalyanmoy, Amrit Pratap, Sameer Agarwal, and T. Meyarivan. 2002. "A Fast Elitist Multiobjective Genetic Algorithm: NSGA II." *IEEE Transactions on Evolutionary Computation* 6(2): 182-197. doi 10.1109/4235.996017.
13. dSPACE INC. 2011. "Microautobox: Hardware Installation and Configuration." Release 7.1.
14. EcoCAR2. 2013. "EcoCAR2 Year Two Event Rules" Revision E. www.ecocar2.org.
15. Environmental Protection Agency (EPA). 2011. www.epa.gov/fueleconomy.
16. Fujita K, et al.1998. "Multi-objective optimal design of automotive engine using genetic Algorithm." *ASME* Design Engineering Technical Conferences.
17. Gen M, and Cheng R. 1997. *Genetic Algorithms and Engineering Design*. John Wiley & Sons. ISBN-13: 978-0471127413.
18. General Motors Corporation. 2005. *Chevrolet Cobalt and Pontiac Pursuit Service Manual*.
19. Gladwin, D., Stewart, P., Stewart, J. 2009. "Internal Combustion Engine Control for Series Hybrid Electric Vehicles by Parallel and Distributed Genetic Programming/Multiobjective Genetic Algorithms." *International Journal of System Science*.doi: 10.1080/00207720903144479.
20. Goldberg E.D. 1953. *Genetic Algorithms in Search, Optimization, and Machine Learning*. Addison-Wesley. ISBN-13: 978-0201157673.

21. Hannan, M.A., Hussain, A., Mohamed, A., Samad, S.A. 2008. “Development of an Embedded Vehicle Safety System for Frontal Crash Detection.” *Internal Journal of Crashworthiness*. 13(5): 579-587. doi: 10.1080/13588260802316714.
22. Ho, Phu, and Eric Klang. 2013. “Intelligent Energy Distribution for Series HEVs Using Determined Optimal Driving Patterns via a Genetic Algorithm.” Technical paper. SAE 2013 World Congress. PN 2013-01-0572.
23. Hooker J.N. 1988. “Optimal Driving for Single-vehicle fuel Economy.” Pergamon Press. GB Transpn. Rcs..A Vol. 22A. No. 3. pp. 183-201.
24. Holland, H. John. 1992. “Genetic Algorithms,” *Scientific American*.
25. Hou, Deyang, et al. 2011. “Spray and Atomization Characteristic of a Micro-Variable Circular-Orifice (MVCO) Fuel Injector.” Conference Article. SAE 2011 World Congress. doi: 10.427/2011-01-0679.
26. Hu,Y., Yurkovich, S., et al. 2011. “Electro-thermal Battery Model Identification for Automotive Applications.” *Journal of Power Sources*. 196(1): 449-457. doi: 10.1016/j.jpowsour.2010.06.037.
27. Incropera, P. F., and David P. Dewitt. 2002. *Fundamentals of Heat and Mass Transfer*. 5th Ed. Wiley. ISBN-10: 0471386502.
28. Ippolito, Lucio, Vincenzo Loia, et al. 2003. “Extended Fuzzy C-means and Genetic Algorithm to Optimize Power Flow Management in Hybrid Electric Vehicles.” *Fuzzy Optim. Decis. Mak*. doi: 10.1023/B:FODM. 03954.49357.b3.
29. Junghwan, R., Yeongseop, P., and Myuongho, S. 2010. “Electric powertrain modeling of a fuel cell hybrid electric vehicle and development of a power distribution algorithm

based on driving mode recognition." *Journal of Power Sources*. doi:10.1016/j.jpowsour.2010.03.081.

30. Karen I, and Yildiz, A.R. 2006. "Hybrid Approach for Genetic Algorithm and Taguchi's Method based design optimization in Automotive industry." *International Journal of Production Research.* 44(22):4897-4914. doi: 10.1080/00207540600619932.
31. Liu, Xudong, Wu, Yanping, Duan, Jianmin. 2008. "Power Split Control Strategy for a Series Hybrid Electric Vehicle Using Fuzzy Logic." *IEEE Int. Conf. Autom. Logist. ICAL*. doi: 10.1109/ICAL.2008.4636199.
32. Michalek, J. J., Panos Papalambros, and Steven J. Skerlos. 2004. "A Study of Fuel Efficiency and Emission Policy Impact on Optimal Vehicle Design Decision." *Journal of Mechanical Design* 126(6): 1062-1070. doi: 10.1115/1.1804195.
33. Moon, C., Kim, J., Choi, G., and Seo, Y. 2002. "An efficient genetic algorithm for the travelling salesman problem with precedence constraints." *European Journal of Operational Research*. doi:10.1016/S0377-2217(01)00227-2.
34. Paladini, V., Teresa Donateo, Srturo de Risi, and Domenico Laforgia. 2007. "Super-capacitors fuel-cell hybrid electric vehicle optimization and control strategy development." *Energy Conversion and Management* 48(11):3001-3008. doi:10.1016/j.enconman.2007.07.014.
35. Plett, L. G. 2004. "Extended Kalman Filtering for Battery Management systems of LiPB-based HEV Battery Packs Part 1. Background." *Journal of Power Sources*. doi: 10.1016/j.jpowsour.2004.02.031.

36. Plett, L. G. 2004. “Extended Kalman Filtering for Battery Management Systems of LiPB-based HEV Battery Packs – Part 3 State and Parameter Estimation.” *Journal of Power Sources*. doi: 10.1016/j.jpowsour.2004.02.033.

37. Roth, E. P. 2007. “Thermal Ramp Abuse Test: Evaluation of Baseline A123 Cells. Sandia National Laboratories.”

38. Saerens, B., J. Vandersteen, T. Persoons, J. Swevers, M. Diehl, and E. Van den Bulck. 2009. “Minimization of the fuel consumption of gasoline engine using dynamics optimization.” *Applied Energy* 86(9):1582-1588. doi:10.1016/j.apenergy.2008.12.022.

39. Sahoohi,Y., and H. Faraneh. 2009. “Model for Developing an Eco-driving Strategy of a passenger vehicle based on the least fuel consumption.” *Applied Energy* 86(10):1925-1932. doi:10.1016/j.apenergy.2008.12.017.

40. Schulz, M. 2004. “Circulatiing Mechanical Power in a Power-Split Hybrid Electric Vehicle Transmission.” Proc. Inst. Mech. Eng. Part D. J. Automob. Eng. doi: 10.1243/0954407042707759.

41. Shaeck, S., Stoermer, A. O., and Hockgeiger, E. 2009. “Micro-hybrid electric vehicle application of valve-regulated lead-acid batteries in absorbent glass mat technology: Testing a partial-state-of-charge operation strategy.” *Journal of Power Sources* 190(1): 173-183. doi:10.1016/j.jpowsour.2008.10.061.

42. Schicbahn, Michael, et al. 2008. “Coordination of Multiple Active Systems for Improved Vehicle Dynamics Controls.” Conference Article, FISITA World Automotive 2008.

43. Schwarzkopf, A.B, and Lbipnik, R.B. 1977. “Control of Highway vehicles for Minimize Fuel Consumption over varying Terrain.” *Pergamon Press Transpn Res*. Vol. II, pp. 279-286.

44. Springs, Peter, Christopher H. Onder, and Lino Guzzella. 2007. “Optimized Control of a Pressure-Wave Supercharger: A Model-Based Feedforward Approach.” *IEEE Control Systems Technology* 15(3):457-464, doi: 10.1109/TCST.2007.894639.

45. Syed, U. Fazal, Kuang, L. Ming, et al. 2006. “Derivation and Experimental Validation of Power-Split Hybrid Electric Vehicle Model.” *IEEE Trans. Veh. Technol.* doi: 10.1109/TVT.2006.878563.

46. Vanderplaats, N. G. 2007. *Multidiscipline Design Optimization*. VR&D, ISBN-13: 978-0944956007.

47. Varesi, K., Randan, A.. 2011. “A Novel Methodology Proposed for Optimizing the Degree of Hybridization in Parallel HEVs Using Genetic Algorithm.” *World Acad. Sci. Eng. Technol.*

48. Wloch K, and Bentley J. P. 2004. “Optimising the Performance of a Formula One Car Using a Genetic Algorithm.” *Springer-Verlag* PPSN VIII, LNCS 3242, pp. 702–711.

49. Woodward. 2011. “Motohawk Control Solutions.” www.mcs.woodward.com.

50. Wu, Lianghong, Wang, Yaonan, et al. 2011. “Multiobjective Optimization of HEV Fuel Economy and Emissions Using the Self-Adaptive Differential Evolution Algorithm.” *IEEE*. doi: 10.1109/TVT.2011.2157186.

51. Wu, B, Prucka, RG, et al. 2005. “Cam phasing optimization using artificial neural network as surrogate models-maximizing torque output.” SAE PN 2005-01-3757.

52. Zeraoulia, M., Benbouzid, M. and Diallo, D. 2006. “Electric Motor Drive Selection Issues for HEV Propulsion Systems: A Comparative Study.” *IEEE*. doi: 10.1190/TVT.2006.878719.

53. Zhao, Jinxing, Xu, Min, et al. 2011. “Design and optimization of an Atkinson cycle engine with the Artificial Neural Network Method.” *Applied Energy*. doi: 10.1016/j.apenergy.2011.11.060.

APPENDIX

Appendix A

Simulink/ADVISOR

The adaptive control strategy model development in Simulink/MATLAB will be covered in this portion of the Appendix. The model is embedded in ADVISOR for the series PHEV architecture with the newly implemented adaptive control strategy. This portion of the Appendix covers the model development process in Simulink/MATLAB and implementation in ADVISOR.

First, the following variables are defined for the adaptive control strategy in the MATLAB workspace:

```
cs_bandwidth_mode1 = 0.15; % 0.1, mode1 set for bandwidth
cs_bandwidth_mode2 = 0.05; % 0.05, mode2 set for bandwidth
cs_threshold_mode1 = 45; % determined via a GA
cs_threshold_mode2 = 62.5; % determined via a GA

cs_lo_soc = 0.2; %(--), lowest desired battery state of charge
cs_hi_soc = 0.8; % (--), highest desired battery state of
charge
```

Starting with the series vehicle architecture (BD_SER) in ADSVISOR as the base vehicle modified the static threshold of the highest and lowest battery SOC to accommodate the adaptive SOC limits. A new model was developed to adapt the lowest and highest desired

battery SOC based on the driving vehicle speed. The newly integrated adaptive control strategy, in blue, is shown in Figure A.1. This block in the model is designed to govern the active state of the ICE (in the model denoted as fc_on 'fuel consumption_on'). The two outputs from the adaptive control strategy replace the two static lowest and highest desired battery SOC limits.

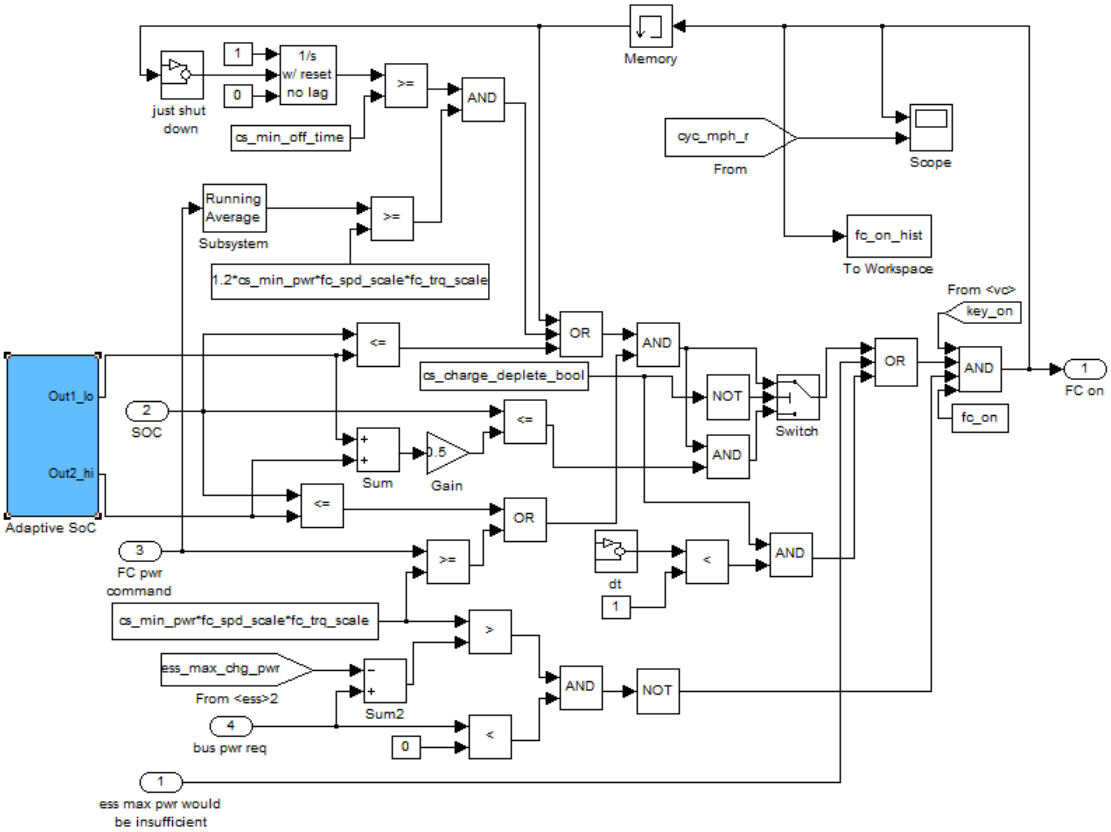

Figure A.1: ICE on Simulink model for adaptive control in ADVISOR with adaptive SOC.

The logic of the control strategy is modeled as shown below.

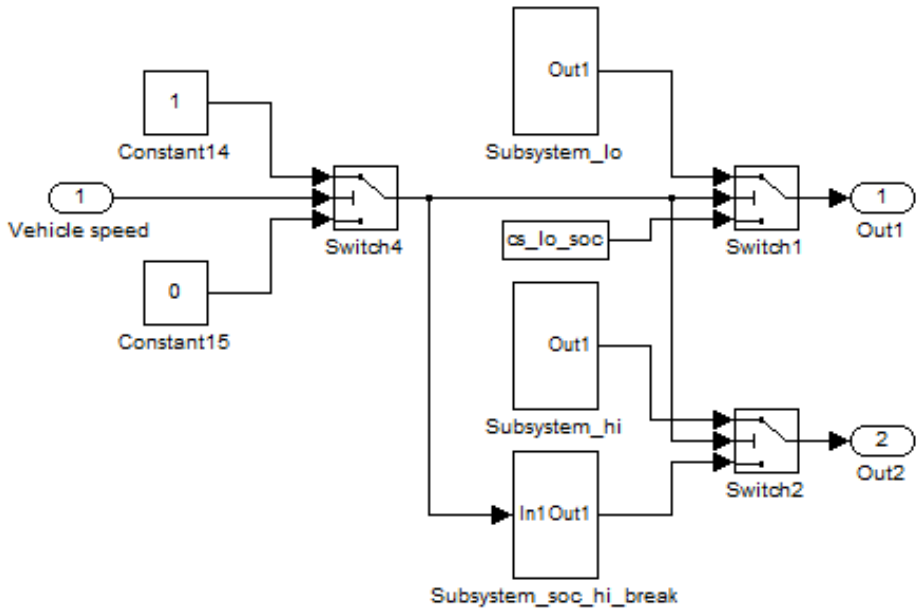

Figure A.2: Adaptive control strategy model in Simulink.

The model uses the vehicle speed as the first logic to define the driving mode (mode1 or mode2). Four basic states are used in the model: adaptive low, adaptive high, cs_lo_soc, and soc_high_break. The adaptive low and adaptive high are active when the if-then conditions are met. When the conditions are no longer satisfied, the logic returns to the static threshold with the value defined by cs_lo_soc. The soc_hi_break function block allows proper exit of the adaptive control when the conditions are no longer satisfied to define the new highest desired battery SOC with cs_hi_soc.

A lag controller is used to define the new upper and lower desired battery SOC limits. The lag controller is used to allow the flexibility to tune the controller based on the vehicle

when implemented. Figure A.3 shows the implementation of the lag controller in the adaptive control strategy.

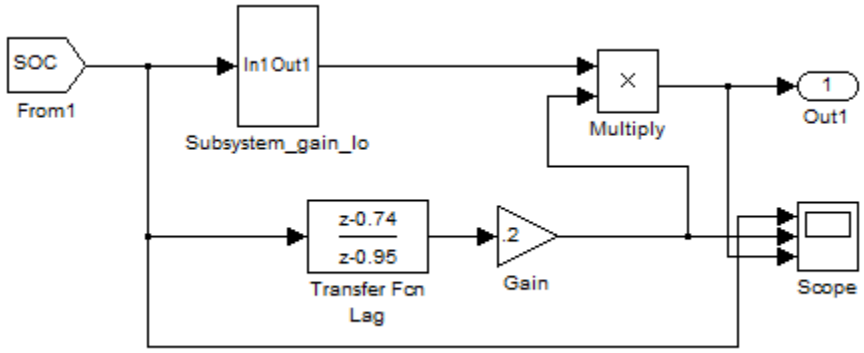

Figure A.3: Lag control implementation in adaptive control strategy.

By having the flexibility to tune the upper and lower to the desirable characteristic, an adaptive control strategy can be achieved. Chapter 4 looks at the different parameters along with tuning preferences to arrive at the desirable controller parameters. This idea can be applied to a control strategy for a series PHEV to improve fuel economy and improve battery life.

Appendix B

Lumped Capacitance

The lumped capacitance model used in determining the thermal characteristic of the ESS will be covered in this portion of the Appendix. Lumped capacitance method is a simple yet commonly used method to solve transient thermal problems. Since the ESS undergoes transient condition during operation, the lumped capacitance thermal model was chosen to determine the average battery temperature as a function of time. The essence of the lumped capacitance method is the assumption that the temperature of the solid is spatially uniform at any instant during the transient process (Incropera & Dewitt 2002). The transient temperature response is based on the overall energy balance on the solid where the heat loss at the surface is equal to the rate of change of the internal energy.

Based on conservation of energy, the total energy stored in the system can be expressed as follows:

$$E_{in} + E_g - E_{out} = \Delta E_{st} \qquad \text{Eq. 1}$$

Where E_{in} and E_{out} is the thermal energy entering and leaving through the control surface. E_g is the energy generation and ΔE_{st} is the rate of change of stored within the controlled volume.

$$E_g - (q^{"}_{cond} + q^{"}_{conv})A_{s(c,cv)} = \rho V c \frac{dT}{dt}$$ Eq. 2

$q^{"}_{cond} + q^{"}_{conv}$ is the conduction and convection heat flux, respectively, A_s is the surface area, ρ is the density, V is the volume, c is the heat capacity. By solving Eq. 2 the temperature can be found as follows:

$$T = \int_0^t \frac{E_g - E_{out}}{\rho V c} dt$$

Eq. 3

T is the temperature at any given time, *t*, of the system. For the ESS analysis, energy in $E_{in} = 0$ and energy generation E_g within the module is calculated through resistance heating.

$$E_g = I^2 R_e$$ Eq. 4

I is the current, R_e is ohmic or resistance heating.

Assumptions:

Battery module:

No temperature gradient within battery module

Charge/Discharge resistance: 0.008Ω

Heat capacity: $c_p = 707 \frac{J}{kg \cdot K}$

Initial state of charge: (SoC) = 0.7

Coulombic efficiency of 0.967

Aluminum housing:

$k = 220 \frac{W}{mK}$

$thickness, t = 0.001\ m$

Air properties:

$h = 5 \frac{W}{m^2 K}$

The total effective thermal resistance is as follows:

$$R_{eff} = \frac{t}{kA} + \frac{1}{hA} = \frac{0.001}{(220 \cdot 0.034)} + \frac{1}{(5 \cdot 0.034)} = 5.88 \frac{W}{m \cdot K}$$

Eq. 5

Heat loss through the aluminum housing for air was done using a single module lumped capacitance model. Where the energy generation per module is $E_{g,mod} = \frac{E_{g,total}}{\#\ module}$ with a single module mass of $21kg$ and cooling surface area, $A_{sur} = 0.034m^2$. The electrical current for the drive cycles was extracted from ADVISOR 2002 and serve as input for the lumped capacitance model. The thermal characteristic of the ESS is then calculated to determine the temperature rise for different driving scenarios.

Appendix C
CAN Setup

This portion of the Appendix covers the configuration for the dbc files for setting up the CAN environment for the ESS and electric drive motor. As mentioned in Chapter 5, the vehicle uses both analog and CAN signals. While analog and digital signals are important, CAN signals can carry a large amount of data with minimum wire requirement, which is of interest for the adaptive control strategy. This section covers the CAN environment that will be utilized by the adaptive control strategy.

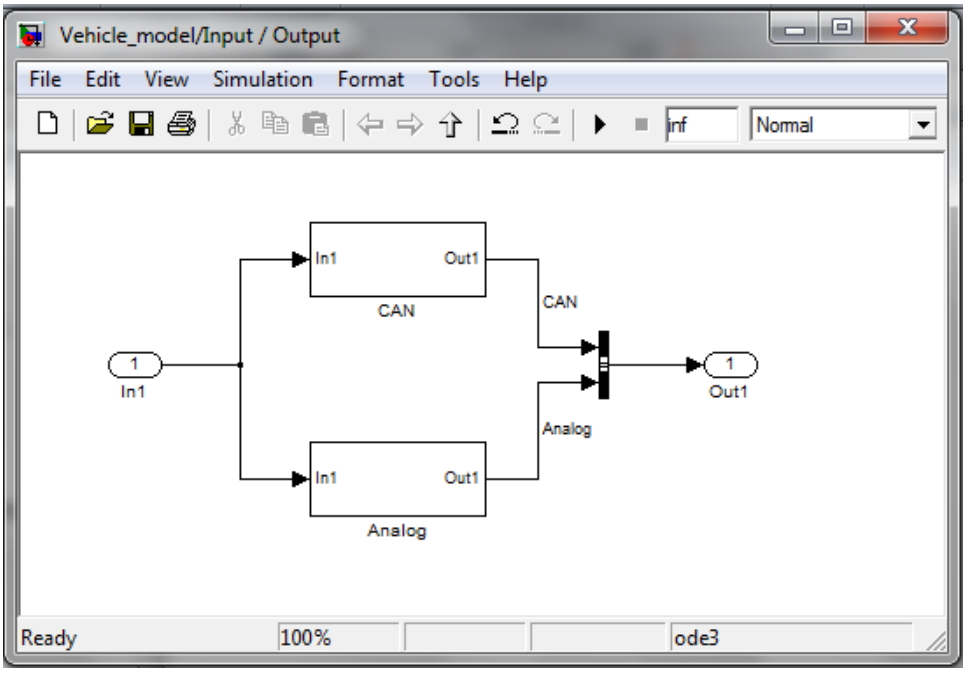

Figure A.4: Vehicle model with analog and CAN input and output.

Figure A.4 shows the layout of the CAN setup for vehicle integration for the NCSU EcoCAR2. As shown Figure A.5, the first block is the CAN controller setup, where the CAN definition assignment can be found. Then the CAN messages from the battery, electric drive motor and the vehicle are channeled into the HS CAN bus. The two main subsystems of interest are the ESS and the electric drive motor. These two subsystems are important because they provide the battery's SOC and vehicle speed, which is used in the adaptive control strategy.

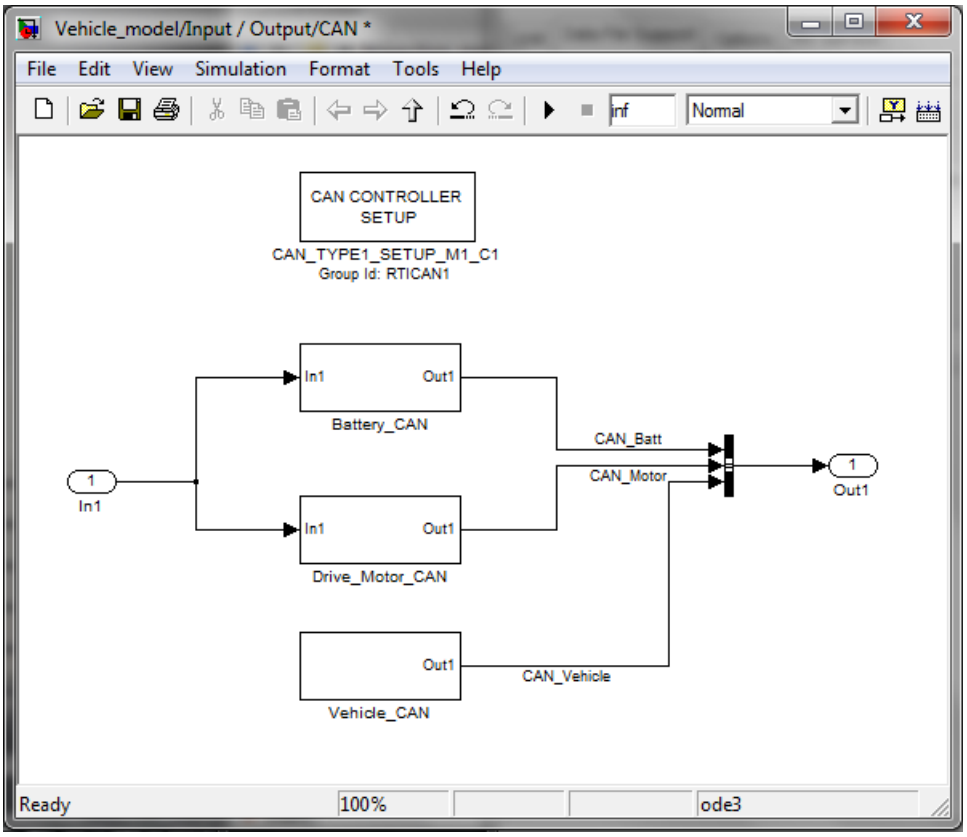

Figure A.5: CAN controller layout for vehicle integration.

The Figure A.6 shows the CAN controller setup for the assignment of the dbc file for the BCM. By defining the dbc file, the CAN message definitions are automatically loaded in the work environment. This provides a simple platform for creating CAN messages in Simulink via predefined CAN block by dSPACE.

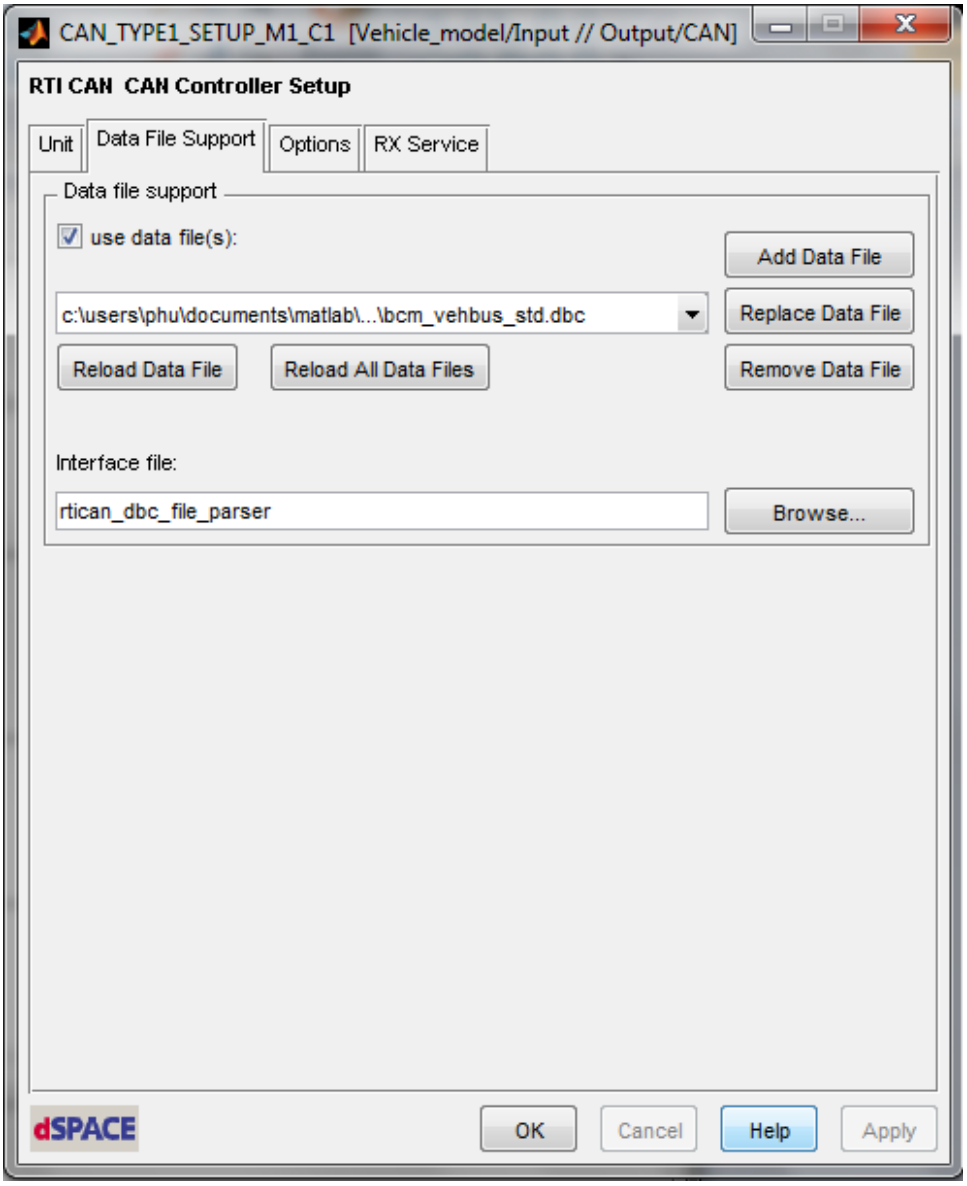

Figure A.6: CAN controller setup in MATLAB for dSPACE.

The Figure A.7 shows the configuration for the received message from the BCM via CAN. This shows the message ID along with the length of the message and how the byte layout is assigned.

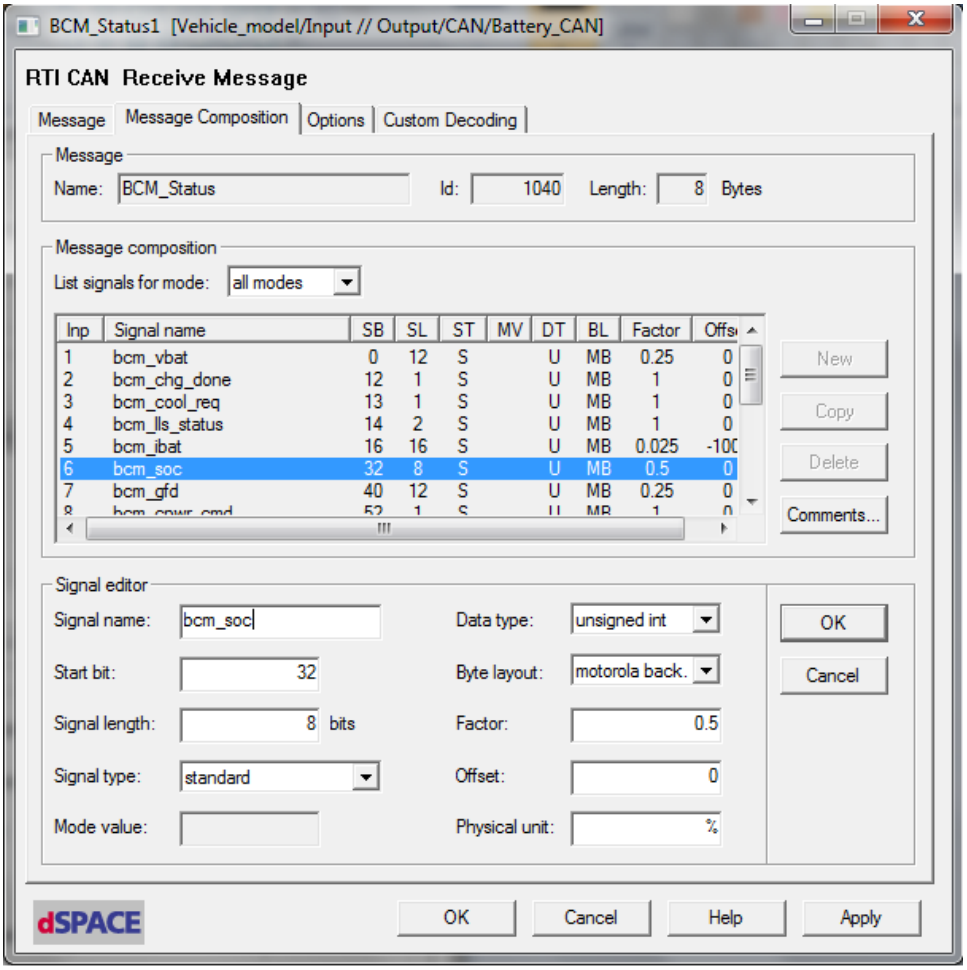

Figure A.7: CAN setup of receiving messages from BCM.

Similarly, the configuration for the CAN transmit message is shown in Figure A.8.

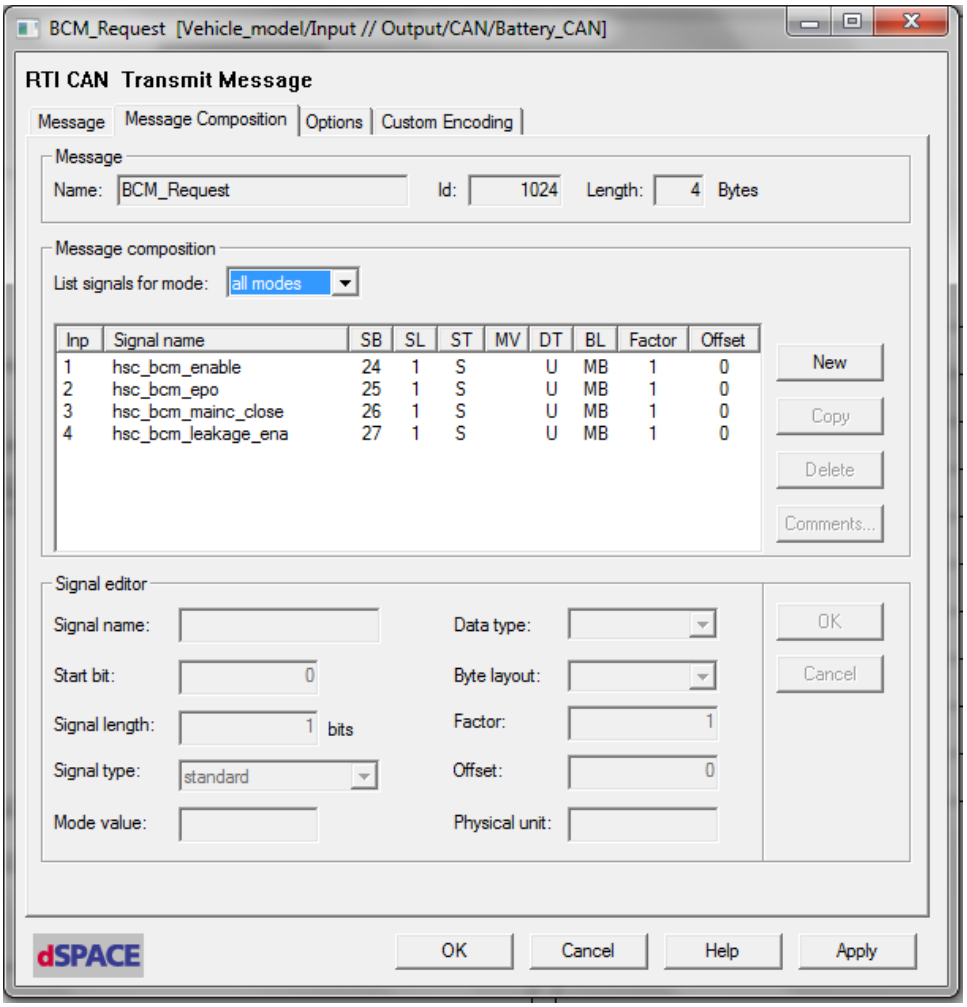

Figure A.8: CAN setup of transmit messages from BCM.

Once these configuration files are setup, we can proceed to build the control model utilizing CAN in Simulink environment. A CAN message can be used as input or output as necessary by the control strategy. By having the dbc file loaded in the workspace, the message definitions are handled automatically, allowing multiple messages to be programmed with ease. Having this flexibility is critical when developing the controls for the vehicle because it requires a large amount of signals. Equally important is the common CAN

communication protocol for different subsystems, allowing controls to integrate with the existing vehicle effortlessly.